

## Adverse Interactions of Luminescent Semiconductor Quantum Dots with Liposomes and *Shewanella oneidensis*

Denise N. Williams, Sunipa Pramanik, Richard P. Brown, Bo Zhi, Eileen McIntire, Natalie V. Hudson-Smith, Christy L. Haynes, and Zeev Rosenzweig

ACS Appl. Nano Mater., Just Accepted Manuscript • DOI: 10.1021/acsanm.8b01000 • Publication Date (Web): 10 Aug 2018

Downloaded from <http://pubs.acs.org> on August 13, 2018

### Just Accepted

“Just Accepted” manuscripts have been peer-reviewed and accepted for publication. They are posted online prior to technical editing, formatting for publication and author proofing. The American Chemical Society provides “Just Accepted” as a service to the research community to expedite the dissemination of scientific material as soon as possible after acceptance. “Just Accepted” manuscripts appear in full in PDF format accompanied by an HTML abstract. “Just Accepted” manuscripts have been fully peer reviewed, but should not be considered the official version of record. They are citable by the Digital Object Identifier (DOI®). “Just Accepted” is an optional service offered to authors. Therefore, the “Just Accepted” Web site may not include all articles that will be published in the journal. After a manuscript is technically edited and formatted, it will be removed from the “Just Accepted” Web site and published as an ASAP article. Note that technical editing may introduce minor changes to the manuscript text and/or graphics which could affect content, and all legal disclaimers and ethical guidelines that apply to the journal pertain. ACS cannot be held responsible for errors or consequences arising from the use of information contained in these “Just Accepted” manuscripts.



ACS Publications

is published by the American Chemical Society, 1155 Sixteenth Street N.W., Washington, DC 20036

Published by American Chemical Society. Copyright © American Chemical Society. However, no copyright claim is made to original U.S. Government works, or works produced by employees of any Commonwealth realm Crown government in the course of their duties.

1  
2  
3  
4  
5  
6  
7 **Adverse Interactions of Luminescent Semiconductor Quantum Dots with Liposomes and**  
8 ***Shewanella oneidensis***  
9

10  
11  
12 Denise N. Williams<sup>1</sup>, Sunipa Pramanik<sup>2</sup>, Richard P. Brown<sup>1</sup>, Bo Zhi<sup>2</sup>, Eileen McIntire<sup>2</sup>, Natalie  
13  
14 V. Hudson-Smith,<sup>2</sup> Christy L. Haynes<sup>2</sup>, and Zeev Rosenzweig<sup>1\*</sup>

15  
16  
17 <sup>1</sup>Department of Chemistry and Biochemistry, University of Maryland Baltimore County,  
18 Baltimore MD 21250  
19

20  
21 <sup>2</sup>Department of Chemistry, University of Minnesota, Minneapolis MN 55455  
22  
23  
24  
25  
26

27  
28 \*Corresponding Author's Email Address: zrosenzw@umbc.edu  
29  
30  
31  
32  
33  
34  
35  
36  
37  
38  
39  
40  
41  
42  
43  
44  
45  
46  
47  
48  
49  
50  
51  
52  
53  
54  
55  
56  
57  
58  
59  
60

## 1 2 3 ABSTRACT 4 5 6 7

8 Cadmium-containing luminescent QD are increasingly used in display, bio-imaging, and energy  
9 technologies; however, significant concerns have been raised about their potentially adverse  
10 impact on human health and the environment. This study makes use of a broad toolkit of  
11 analytical methods to investigate and increase our understanding of the interactions of  
12 luminescent cadmium-containing (CdSe) and cadmium-free (ZnSe) quantum dots (QD), with  
13 and without a passivating higher bandgap energy ZnS shell, with phospholipid vesicles  
14 (liposomes), which model bacterial membranes, and with *Shewanella oneidensis* MR-1, an  
15 environmentally relevant bacteria. A unique feature of this study is that all QD types have the  
16 same surface chemistry, being capped with uncharged polyethylene glycol (PEG) ligands. This  
17 enables focusing the study on the impact of the QD core on liposomes and bacterial cells. The  
18 study reveals that QD association with liposome and bacterial cell membranes is imperative for  
19 their adverse impact on liposomes and bacterial cells. The QD concentration dependent  
20 association with liposomes and bacteria destabilizes the membranes mechanically, and leads to  
21 membrane disruption and lysis in liposomes, and to bacterial cell death. The study also shows  
22 that cadmium-containing QD exhibit a higher level of membrane disruption in bacterial cells  
23 than cadmium-free QD. ZnSe QD have low membranal impact and coating them with a ZnS  
24 shell decreases their membrane disruption activity. In contrast, CdSe QD exhibit a high level of  
25 membranal impact, and coating them with a ZnS shell does not decrease, but in fact further  
26 increases their membrane disruption activity. This behavior might be attributed to higher  
27 affinity and association of CdSe/ZnS QD with liposomes and bacterial cells, and to a  
28 contribution of dissolved zinc ions from the ZnS shell to increased membrane disruption  
29 activity.  
30  
31  
32  
33  
34  
35  
36  
37  
38  
39  
40  
41  
42  
43  
44  
45  
46  
47  
48  
49  
50  
51  
52  
53  
54  
55  
56  
57  
58  
59  
60

Keywords: quantum dots, liposomes, *Shewanella oneidensis* MR-1, membrane association, membrane disruption

## INTRODUCTION

In the last two decades luminescent semiconductor quantum dots (QD) have been incorporated into a broad range of applications including bio-imaging, solar cells, and display technologies.<sup>1-7</sup> Luminescent QD provide an attractive alternative to organic fluorophores in these applications because of their unique optical properties, including broad absorption peaks with high molar extinction coefficients, size-dependent narrow emission peaks, high emission quantum yield, and high chemical stability and photostability.<sup>8</sup> Historically, cadmium and lead-containing QD have been widely used because of their excellent photo-physical properties and relatively simple syntheses.<sup>1, 9, 10</sup> However, concerns about the broad use of toxic metal-containing nanomaterials have limited large-scale development and use of QD technologies, and led to efforts to replace cadmium and lead-containing QD with alternative non-toxic QD.<sup>10-12</sup> For example, ZnSe QD have been explored as a non-toxic alternative to CdS and CdSe QD.<sup>7, 13, 14</sup> This substitution comes with ease since ZnSe QD are structurally similar and prepared using the same synthetic methodology as CdSe QD. This enables us to replace cadmium with zinc in the QD cores while maintaining the same surface chemistry for all four QD types used in our study. It should be noted that other optical nanomaterials, for example, InP<sup>15</sup>, graphene<sup>16</sup>, and silicon<sup>17</sup> QD have been explored as nontoxic alternatives to cadmium-containing QD in QD-based technologies, but variations in their surface chemistry make it difficult to compare their impact on liposomes and cells.<sup>18</sup>

To date, a number of toxicity studies have demonstrated that ZnSe QD are less toxic than their cadmium-containing counterparts.<sup>12, 19</sup> The adverse effects of cadmium-containing QD on cells and organisms were attributed to a combination of factors including the association of the QD with cell membranes, QD ion dissolution, and reactive oxygen species (ROS) generation (particularly when the QD are irradiated with a UV light); all factors with the capability to negatively impact model membranes and bacterial cells.<sup>12, 19</sup> Several studies have found that coating luminescent semiconductor QD with a higher energy bandgap shell decreases the toxicity of cadmium-containing QD towards cells and living organisms by inhibiting ROS generation and ion dissolution.<sup>15, 20-22</sup> Other studies revealed that coating cadmium-containing QD with a passivating shell only delays adverse interactions of luminescent QD with cells and

1  
2  
3 living organisms.<sup>21, 23-28</sup> Cadmium dissolution is often described as a main contributor to QD  
4 toxicity.<sup>21, 28-30</sup> In contrast, the role of zinc dissolution from commonly used CdSe/ZnS QD has  
5 not been considered as a main contributor to the toxicity of cadmium-containing QD since the  
6 ZnS shell is often assumed to be inert.<sup>25</sup>  
7  
8

9  
10 Our study describes the interactions between luminescent CdSe and ZnSe QD with  
11 phospholipid vesicles (liposomes), which model the membrane of gram-negative bacteria, and  
12 with *Shewanella oneidensis* MR-1, an environmentally relevant gram-negative bacterium which  
13 is often used as a model organism for bioremediation research due to its metal-reducing  
14 capabilities.<sup>31, 32</sup> ZnSe, ZnSe/ZnS, CdSe and CdSe/ZnS QD were synthesized using nearly  
15 identical synthesis methods to insure that the QD have the same surface chemistry and only  
16 differ in their cores. The synthesis, characterization, and careful control of surface chemistry of  
17 luminescent QD, rather than relying on commercially available QD with unknown surface  
18 content, is imperative to understand their interactions with model membranes and bacterial  
19 cells. Our study reveals that cadmium-containing QD have greater membrane disruption activity  
20 than cadmium-free QD, most likely due to increased membrane association and a higher rate of  
21 ion dissolution which destabilizes the liposome and bacterial cell membranes. Surprisingly,  
22 coating QD with a ZnS shell does not always decrease their membrane disruption activity. In  
23 CdSe/ZnS QD, structural irregularities, particularly when the QD are coated with a thick shell,  
24 lead to an increased dissolution rate of the ZnS shell. While zinc ion control measurements  
25 reveal that the liposomes are stable in the presence of zinc ions in the sample solutions, it is still  
26 possible that the increased rate of zinc ion dissolution adversely impact the membrane of  
27 liposomes and bacterial cells when the CdSe/ZnS QD dissolve after they associated with the  
28 liposome or cell membranes.  
29  
30  
31  
32  
33  
34  
35  
36  
37  
38  
39  
40  
41  
42  
43  
44  
45  
46  
47  
48  
49  
50  
51  
52  
53  
54  
55  
56  
57  
58  
59  
60

1  
2  
3 MATERIALS AND METHODS  
4  
5  
67  
8  
9  
10  
11  
12  
13  
14  
15  
16  
17  
18  
19  
20  
21  
22  
23  
24  
25  
26  
27  
28  
29  
30  
31  
32  
33  
34  
35  
36  
37  
38  
39  
40  
41  
42  
43  
44  
45  
46  
47  
48  
49  
50  
51  
52  
53  
54  
55  
56  
57  
58  
59  
60  

**Reagents.** Zinc stearate (ZnSt), 1-dodecylphosphonic acid (DPA, 95%), zinc formate (98%), and zinc acetate were purchased from Alfa Aesar. 1-Octadecene (ODE), diphenyl phosphine (DPP), sulfur powder, trioctylphosphine (TOP, 97%), tetramethylammonium hydroxide solution (TMAH, 25 wt.% in methanol), tetradecylphosphonic acid (97%), cadmium acetylacetonate (CdAcAc, 99.9%), sodium chloride, LUDOX TMA colloidal silica (34 wt. % suspension in H<sub>2</sub>O), and hexamethyldisilathiane ((TMS)<sub>2</sub>S, synthesis grade) were purchased from Sigma Aldrich. Selenium powder (Se, 99.5%), 1-hexadecylamine (HDA, 90%), oleylamine (C<sub>18</sub> content 80-90%), and sodium hydroxide were purchased from Acros Organic. BD Difco™ Dehydrated Culture Media: LB Broth, Dulbecco's Phosphate-Buffered Saline (without calcium and magnesium), BD Difco™ Dehydrated Culture Media: Granulated Agar, Corning Cellgro DPBS (1X), chloroform, toluene, methanol, HEPES Buffer (1M), and nitric acid (Trace Metal Grade) were purchased from Fisher Scientific. Instrument Calibration Standard 2 (5% HNO<sub>3</sub>/Tr. Tart. Acid/ Tr. HF) for inductively coupled plasma mass spectrometry (ICP-MS) was purchased from Claritas PPT SPEX CertiPrep. DHLA-PEG750-OCH<sub>3</sub> was prepared and purified with slight modifications to a previously reported protocol.<sup>33, 34</sup> 1-palmitoyl-2-oleoyl-sn-glycero-3-phosphocholine (POPC), 1-palmitoyl-2-oleoyl-sn-glycero-3-phospho-(1'-rac-glycerol) (sodium salt) (POPG), and 1,2-dioleoyl-sn-glycero-3-phosphoethanolamine-N-(7-nitro-2-1,3-benzodiazol-4-yl) (ammonium salt) (NBD-POPE) were purchased from Avanti Polar Lipids, Inc. Calcein disodium salt (calcein) was purchased from Fluka. *Shewanella oneidensis* MR-1 BAA-1096 was purchased from American Type Culture Collection.

43  
44  
45  
46  
47  
48  
49  
50  
51  
52  
53  
54  
55  
56  
57  
58  
59  
60  

**ZnSe and ZnSe/ZnS QD Synthesis.** ZnSe and ZnSe/ZnS QD were synthesized according to a previously reported procedure.<sup>14</sup> The reaction was carried out in a 25 ml three-neck round bottom flask under stirring. The zinc precursor solution was prepared in the round bottom flask by dissolving 632 mg (1 mmol) ZnSt powder in 5.0 mL of ODE at 120°C under inert nitrogen gas. The three-neck flask was vacuumed out for 30 minutes and then backfilled with nitrogen gas while heating the solution to 280°C. A selenium precursor solution was prepared by dissolving 7.9 mg selenium powder in a solution containing 17 µl DPP and 670 µL toluene (selenium concentration of 0.15 M). This selenium solution was injected rapidly into the

reaction mixture and allowed to react for 5 minutes at 280°C before cooling the flask to room temperature. A second selenium precursor solution was prepared by dissolving 78.9 mg selenium powder in 800  $\mu$ l TOP (selenium concentration of 1.0 M). This selenium precursor solution was injected into the reaction mixture at room temperature. The reaction mixture was heated and kept at 280°C for 20 minutes, then cooled down to room temperature. The formed ZnSe QD were immediately coated with a ZnS shell or stored in their reaction mixture at room temperature and away from light. Two precursor solutions were prepared for the ZnS shelling: 1) 32.1 mg sulfur powder in 1 ml TOP (sulfur concentration of 1.0 M), and 2) 632 mg (1.0 mmol) of zinc stearate dissolved in 8 ml ODE. The ZnS shell precursor solutions were injected into the reaction mixture at room temperature. The reaction mixture was then heated, kept at 280 °C for 20 minutes, and finally cooled to room temperature. The resulting ZnSe/ZnS QD were stored in the reaction mixture at room temperature and away from light. Prior to their immediate future use, QD were washed multiple times to remove excess reactants.

**CdSe and CdSe/ZnS QD Synthesis.** CdSe QD were synthesized according to a previously reported procedure.<sup>35</sup> The reaction was carried out in a 50 ml three-neck round bottom flask under stirring. A cadmium precursor solution was prepared by dissolving 5.0 grams hexadecylamine in a 10 ml TOP solution that also contained 2.1 mmol tetradecylphosphonic acid, and 1.0 mmol of CdAcAc. The solution was heated to 100°C under inert nitrogen gas for the reactants to fully dissolve. The flask was vacuumed out for 30 minutes then backfilled with nitrogen gas. The solution was heated to 250°C, cooled back down to 100°C and vacuumed again for 30 minutes. After backfilling with nitrogen, the vessel was heated to 300°C. A 5 ml selenium precursor solution, which contained 0.84 M selenium powder in TOP, was injected rapidly into the reaction mixture. The CdSe QD formed instantly and the reaction mixture was cooled to 80°C for overnight annealing. The resulting CdSe QD were stored in the reaction mixture at room temperature and away from light. CdSe/ZnS QD were synthesized using successive ionic layer adsorption and reaction (SILAR). SILAR calculation and shelling was carried out following a previously described protocol where 0.3nm radius monolayers of a ZnS shell are added one at a time.<sup>36</sup> 0.15  $\mu$ moles of washed CdSe QD were added to a solution that contained 6 ml ODE, 4 ml TOP, 6 ml oleylamine, and 10 mg of dodecylphosphonic acid in a 50 ml round bottom flask under nitrogen gas. The solution was heated and kept at 100°C under

1  
2  
3 high vacuum. The flask was backfilled with nitrogen gas. Then, the first aliquot of zinc  
4 precursor (0.05 M zinc formate in oleylamine), which was calculated from the core size to add a  
5 0.3 nm radius monolayer of a ZnS shell, was injected over 15 minutes. The reaction mixture  
6 was heated and kept at 160°C, and an aliquot of sulfur precursor (0.25 M (TMS)<sub>2</sub>S in TOP) was  
7 injected over 15 minutes to form the first monolayer of ZnS shell. The QD were then annealed  
8 at 160°C for 20 minutes. The reaction mixture was heated and kept at 170°C while the process  
9 of adding zinc and sulfur precursors over 15 minutes and annealing over 20 minutes was  
10 repeated. The shelling process was repeated, each time at 10°C higher temperature until the  
11 desired ZnS shell thickness was realized. Finally, the reaction mixture was heated and kept at  
12 200°C and 0.5 ml oleic acid was added dropwise over one hour. The reaction mixture was then  
13 allowed to slowly cool to room temperature.  
14  
15  
16  
17  
18  
19  
20  
21  
22  
23

24 **Capping Luminescent QD with DHLA-PEG750-OCH<sub>3</sub> Ligands.** Luminescent QD were  
25 capped with DHLA-PEG750-OCH<sub>3</sub> ligands (MW= 927 g/mol) to enable their aqueous solution  
26 miscibility. The ligand exchange process used to prepare the DHLA-PEG750-OCH<sub>3</sub> coated QD  
27 removed some TOPO ligands from the QD surface and shield the remaining ones from  
28 interacting with liposome membranes and bacterial cells.<sup>37</sup> This is an imperative step to  
29 minimize the ligand contribution to QD toxicity since TOPO ligands have been shown to be  
30 highly toxic.<sup>38</sup> The ligand exchange was carried out by following a previously reported  
31 procedure.<sup>39</sup> The DHLA ligand (0.25 mmol), 0.5 mmol sodium hydroxide, 0.13 mmol zinc  
32 acetate, and 1 mL of methanol were sonicated together in a septum-closed vial filled under  
33 nitrogen gas. 10 nmol of purified QD were dissolved with a minimal amount of chloroform,  
34 dried under vacuum, and put under a flow of nitrogen. The DHLA ligand solution was added to  
35 the QD solution, and then left overnight at 50 °C under nitrogen gas. The next day 1 mL of  
36 ethyl acetate and enough hexane to separate solvents into two distinct layers were added to the  
37 QD, stirred, and allowed to separate. The hexane layer was removed to waste. The QD in the  
38 ethyl acetate layer were dried under vacuum, and then dispersed in Millipore water. The QD  
39 solution was passed through a 0.45 SFCA syringe filter into a 30,000 MWCO spin filtration  
40 device for washing using three centrifugation cycles at 2000xg for 5 minutes at room  
41 temperature.  
42  
43  
44  
45  
46  
47  
48  
49  
50  
51  
52  
53  
54

**Absorbance and Fluorescence Instrumentation.** UV-Vis absorption spectra were obtained using a Thermo Scientific Evolution 201 UV-Vis spectrophotometer. Fluorescence spectroscopy measurements were carried out using a PTI-Horiba QuantaMaster 400 fluorimeter, equipped with an integration sphere for emission quantum yield measurements, and with a PicoMaster TCSPC detector for fluorescence lifetime measurements. A Molecular Devices SpectraMax M5 Microplate reader was used to observe of changes in fluorescence emission over time.

**Preparation of Calcein-Containing Liposomes.** 10:1 molar POPC: POPG liposomes filled with calcein dye were prepared via a dehydration/rehydration method.<sup>40</sup> In a 500 mL round bottom flask, 2 mL of 25 mg/mL POPC and 0.50 mL of 10 mg/mL POPG in chloroform were stirred together under nitrogen gas to create a dry phospholipid film. The flask was further vacuumed overnight to remove all organic solvent. A 5 mL stock solution containing 5 mM calcein disodium salt in 2 mM HEPES and 25 mM sodium chloride at pH 7.4 was prepared. 3 mL of the calcein solution was added to the dried lipids. The flask was immersed in dry ice-acetone bath until the solid film began to dissociate from the bottom of the flask. The flask was then placed in a water bath at room temperature to form the liposomes. This process was repeated ten times to ensure dye encapsulation in the liposomes. 1 mL of the liposome solution was extruded 15 times through an Avanti Polar Lipids 50 nm pore mini extruder with a polycarbonate membrane. The liposome sample was then run through a Sepharose CL-4B silica column (10 mm x 100 mm) with free HEPES buffer to remove free fluorophore molecules from the dye-containing liposomes.

**Calcein-Containing Liposomes Lysis Assays.** Liposome lysis analysis used the time-based function of the PTI-Horiba QuantaMaster 400 fluorimeter. The excitation wavelength was set to 480 nm, the absorbance maximum of the dye. The emission of calcein was observed at 515 nm, until the fluorescence intensity stabilized typically after 15 minutes. The emission of leaked calcein after interactions with each test sample was observed for 20 minutes total, with stirring, at these parameters: 1-2 minutes to determine background fluorescence of liposomes, 15

1  
2  
3 minutes for substrate to interact with liposomes, 2-3 minutes for maximum liposome lysis to be  
4 determined after a 40  $\mu$ L injection of 1% Triton X-100 in Millipore water.  
5  
6  
7

8 **Preparation of Dye-Free Liposomes.** 10:1 molar POPC: POPG dye-free liposomes were  
9 prepared via the same methods, with the exception that lipids dried overnight were hydrated  
10 with 3mL of 2 mM HEPES and 25 mM sodium chloride solution, followed by  
11 dehydration/rehydration and extrusion.  
12  
13

14  
15  
16 **Preparation of NBD-labeled Liposomes.** 10:1:0.1 molar POPC: POPG:NBD-POPE liposomes  
17 were prepared for a ~1% mol ratio of labeled to unlabeled lipids.<sup>41</sup> In a 250 ml round bottom  
18 flask, 400  $\mu$ L of 25 mg/mL POPC, 100  $\mu$ L of 10 mg/mL POPG, and 100  $\mu$ L of 10 mg/mL  
19 NBD-POPE in chloroform were stirred together under nitrogen gas to create a dry phospholipid  
20 film. The flask was further vacuumed overnight to remove all organic solvent. The next day,  
21 7.5mL of 2 mM HEPES and 25 mM sodium chloride at pH 7.4 was used to hydrate the lipids to  
22 a 2mM lipid concentration. The flask was taken through ten freeze/thaw cycles. Finally, 1 mL at  
23 a time, the liposome solution was extruded 15 times through an Avanti Polar Lipids 50 nm pore  
24 mini extruder with a polycarbonate membrane.  
25  
26

27  
28 **NBD-labeled Liposomes Fluorescence Lifetime Assays.** NBD-labeled liposome steady state  
29 fluorescence was observed from 495-650nm, with the excitation wavelength set to 470 nm. The  
30 fluorescence lifetime of the dye was observed at 515 nm.<sup>42</sup> Steady state and emission readings  
31 were conducted of the NBD-labeled liposomes alone, immediately after the addition of 0.5nM  
32 QD, 4 hours after the addition, and 8 hours after the addition. Only data for 4 hours after the  
33 addition of QD is shown.  
34  
35

36 **Bacterial Culture and Colony Counting when Exposed to QD.** *Shewanella oneidensis* MR-1  
37 bacteria were cultured by streaking an LB-agar plate with bacteria and then incubating the plate  
38 in a 30 °C incubator overnight. Liquid cultures were grown by transferring colony inoculants  
39 from the plate to 10 mL of LB broth and incubating for 4 hours at 30 °C in an orbital shaker, to  
40 their mid-log phase. Cells were then harvested by centrifugation for 10 minutes at 2000xg,  
41 washed in Dulbecco's phosphate-buffered saline (D-PBS) buffer, and suspended in a HEPES  
42  
43

1  
2  
3 buffer (2 mM HEPES and 25 mM NaCl, at pH 7.4). The cultures were then diluted to 0.2 OD at  
4 600 nm (OD600) to achieve a cell density of approximately  $2 \times 10^8$  colony-forming units  
5 (CFUs) /mL. Serial 10-fold dilutions of this bacterial suspension were performed to achieve a  
6 cell concentration of  $10^4$  CFUs/mL in HEPES buffer. The resultant diluted bacteria suspension  
7 was treated with QD, in a total volume of 150  $\mu$ L, at varying concentrations. The QD-exposed  
8 cells were incubated on rotary shaker for 15 minutes, and then the viability of *Shewanella*  
9 *oneidensis* MR-1 bacteria was determined using a drop-plate colony-counting protocol.<sup>43</sup> Six 10  
10  $\mu$ L droplets of the exposed bacterial suspensions and untreated negative controls were dropped  
11 on an LB-agar plate, which were pre-sterilized under UV-illumination for 20 minutes. The  
12 droplets were dried under air flow in a biological cabinet, and then incubated at 30°C for 20  
13 hours before colonies were counted using a Bantex Colony Counter 920A.  
14  
15  
16

17  
18  
19  
20  
21  
22  
23  
24 **Inductive Couple Plasma Mass Spectrometry (ICP-MS) of QD, QD Ion Dissolution, and**  
25 **QD Association with Bacteria.** Inductive coupled plasma mass spectrometry (ICP-MS)  
26 measurements of QD, bacteria, and QD-bacterial samples were carried out using a PerkinElmer  
27 NexION 300D single quad mass spectrometer. The Instrument Calibration Standard 2 was used  
28 daily to prepare calibration curves from 0.1 ppb to 1 ppm for the different ion analytes  
29 (cadmium, selenium, zinc) which could be generated from dissolving the QD. Sample  
30 preparation for ICP-MS analysis was as follows: For QD in organic solvents, QD sample at  
31 predetermined concentration in chloroform was put into a scintillation vial containing acetone  
32 and centrifuged to precipitate out the QD. The QD were allowed to dry, nitric acid was added to  
33 dissolve the sample, and then Millipore water was added to QD-nitric mixture to dilute nitric  
34 acid concentration to 2% by volume. For QD in aqueous solution, QD samples of predetermined  
35 concentrations were dissolved by adding nitric acid to the solution. The solution was kept at  
36 room temperature overnight. Millipore water was added to the QD-nitric acid mixtures to dilute  
37 the nitric acid concentration to 2% by volume and a total sample volume of at least 5 mL. For  
38 investigation of QD dissolution, known concentrations of QD solution were centrifuged through  
39 30,000 MWCO spin filtration devices at 2000xg and the supernatant analyzed for ion content.  
40 The level of association of QD with *Shewanella oneidensis* was determined using ICP-MS  
41 measurements as follows: *Shewanella oneidensis* bacterial cells were cultured in Luria-Bertani  
42 (LB) broth overnight. The resulting bacterial suspension was centrifuged for 10 min at 2000xg,  
43  
44  
45  
46  
47  
48  
49  
50  
51  
52  
53  
54  
55  
56  
57  
58  
59  
60

washed in Dulbecco's phosphate-buffered saline (D-PBS) buffer, suspended in a HEPES buffer (2 mM HEPES and 25 mM NaCl, at pH 7.4) and the OD was adjusted to 0.8 at 600 nm (OD600). The diluted bacterial suspension was treated with CdSe and CdSe/ZnS QD at concentrations equivalent to Cd core concentrations of 0.5 mg/L, 1 mg/L and 2mg/L. Similarly, the treatment concentrations used for the ZnSe and ZnSe/ZnS QDs were equivalent to Zn core concentrations of 1mg/L, 2mg/L and 5 mg/L. After an exposure time of 15 mins for the bacteria and QDs, the cells were harvested as pellets by centrifugation at 2000xg for 10 min. At this low speed of centrifugation only bacterial cells were precipitated along with associated QD, and free QD in the supernatant were discarded. The QD-treated bacterial cell pellets were analyzed with ICP-MS to determine the levels of cadmium and zinc, to confirm QD association with bacterial cells.

**Hyperspectral Imaging of CdSe and CdSe/ZnS QD and Bacteria.** Images of *Shewanella oneidensis* MR-1 bacteria following incubation with CdSe or CdSe/ZnS QD were acquired using high S/N ratio, dark-field Cytoviva® hyperspectral imaging (HSI) (Cytoviva®, Auburn, AL). In these experiments, sample solutions were drop-cast (~3-4  $\mu$ L) onto a glass slide, which was then sealed with a cover slip and clear nail polish. Slides were examined at 100X magnification with an oil immersion lens under an Olympus BX-41 microscope. Spectral data were acquired with a Cytoviva® spectrophotometer and integrated CCD camera in both the visible and near-infrared range (400-1000 nm). Analysis of the HSI spectra was performed by the Environment for Visualization software (ENVI 4.4 version). Spectral libraries of CdSe and CdSe/ZnS QD and *Shewanella oneidensis* MR-1 bacteria were used to help analyze HSI spectral angle mapper (SAM) spectral patterns and characterize association of the QD with the bacterial cells.

**High Resolution Transmission Electron Microscopy of QD.** High resolution transmission electron microscopy (HR-TEM) images of QD were obtained using a Titan 80-300 S/TEM, operating at 300 kV with a Gatan OneView imaging camera. QD samples were drop coated onto mesh copper grids with ultrathin carbon film on holey carbon support film (Ted Pella, Inc.) Grids were then placed in vacuum oven overnight before analysis.

**Biological Transmission Electron Microscopy of Bacteria Incubated with QD.** Biological transmission electron microscopy (BioTEM) images of bacteria exposed to QD were obtained using a FEI Tecnai T12 TEM after the following preparation. *Shewanella oneidensis* bacteria were cultured in LB broth overnight. The next day, bacteria were washed with DPBS buffer, diluted to an OD of 0.8 (OD600) in HEPES, then exposed 1mg/L of CdSe/ZnS QD for 15 minutes. This bacterial suspension was centrifuged down to a pellet, washed thrice with 0.1 M cacodylate buffer solution, then resuspended in a fixation buffer of 2.5% glutaraldehyde in 0.1 M sodium cacodylate buffer and fixed for 50 minutes. The fixed bacterial cells were then centrifuged, washed with sodium cacodylate buffer, and dehydrated stepwise with increasing concentration of ethanol (30, 50, 70, 80, 90, 95, and 100% ethanol in water). After the ethanol rinsing steps, the pellet was washed with propylene oxide three times. The resin infiltration steps were performed in the following manner. The pellet was soaked first in a 2:1 propylene oxide: epoxy resin mixture for 2 h, and then in a 1:1 propylene oxide: epoxy resin mixture overnight. Next day, the 1:1 propylene oxide: epoxy resin mixture was removed and replaced with a fresh batch of 1:1 propylene oxide: epoxy resin mixture for 5 h, and finally incubated in a pure resin mixture and infiltrated overnight. The resin sample was then cured in a 40 °C oven for one day and then 60 °C oven for two days. Leica UC6 microtome and Diatome diamond knife was used to make ultrathin sections (65 nm) of this resin-embedded bacterial sample, and uranyl acetate and lead citrate was used to stain them. These sections were placed on copper TEM grids (Ted Pella Inc.).

## RESULTS AND DISCUSSION

**Characterization of Cadmium-Containing and Cadmium-Free QD.** Cadmium-containing CdSe and cadmium-free ZnSe QD were synthesized by the commonly used “hot injection” method.<sup>14, 35</sup> The CdSe and ZnSe QD were coated with a ZnS shell following previously reported procedures.<sup>14, 36</sup> UV-Vis absorption and emission spectra of CdSe and CdSe/ZnS QD are shown in Figure 1A. The UV-Vis absorption spectra show excitation peaks at 505 nm for CdSe QD, and a red-shifted excitation peak at 552 nm for CdSe/ZnS QD. The emission spectra show corresponding emission peaks at 522 nm for CdSe QD and 580 nm for CdSe/ZnS QD. The emission quantum yields of CdSe and CdSe/ZnS QD were measured to be 13% and 43%, respectively. The full peak width at half maximum (FWHM) of CdSe and CdSe/ZnS QD were 27 and 34 nm, respectively. The UV-Vis absorption and emission spectra for ZnSe and ZnSe/ZnS QD are shown in Figure 1B. The UV-Vis absorption spectra show excitation peaks at 410 and 418 nm for ZnSe and ZnSe/ZnS QD, respectively. The emission spectra show corresponding emission peaks at 418 for ZnSe QD and 423 nm for ZnSe/ZnS QD. The emission quantum yields of the ZnSe QD and ZnSe/ZnS QD were 5% and 10%, respectively. The FWHM of the ZnSe QD and ZnSe/ZnS QD were 17 and 15 nm, respectively. Time-resolved photoluminescence measurements were also carried out to determine the impact of the ZnS shell on the cadmium-containing and cadmium-free QD (see supporting information for details). The fluorescence lifetime of CdSe QD was  $29.6 \pm 0.4$  nsec. It decreased to  $16.9 \pm 1.0$  nsec when the CdSe QD were coated with a ZnS shell to form CdSe/ZnS QD. The fluorescence lifetime of ZnSe QD was  $7.4 \pm 0.3$  nsec. It decreased to  $6.4 \pm 0.1$  nsec when the ZnSe QD were coated with a ZnS shell to form ZnSe/ZnS QD. This decrease in fluorescence lifetime when core QD are passivated with a higher energy bandgap ZnS shell is attributed to increased confinement of the excited electrons in the core QD and is consistent with previous studies.<sup>44</sup> The distinct excitonic peaks in the UV-Vis spectra, the narrow and symmetric emission peaks, and the increase in emission quantum yield with a corresponding decrease in fluorescence lifetime when the QD are passivated with a higher energy bandgap shell suggest that both the cadmium-containing CdSe and CdSe/ZnS QD, and the cadmium-free ZnSe and ZnSe/ZnS QD are of high quality, and display the photo-physical properties required in luminescent QD-based applications.

A ligand exchange reaction was carried out to replace the organic capping ligands of the QD with uncharged DHLA-PEG750-OCH<sub>3</sub> ligands (Scheme 1). This allowed the QD to be dispersed in aqueous media and made them suitable for the liposome lysis and bacterial viability assays. More importantly, the use of the same capping ligand in all four QD types enabled direct comparison between the membrane disruption activity of cadmium-containing and cadmium-free QD.

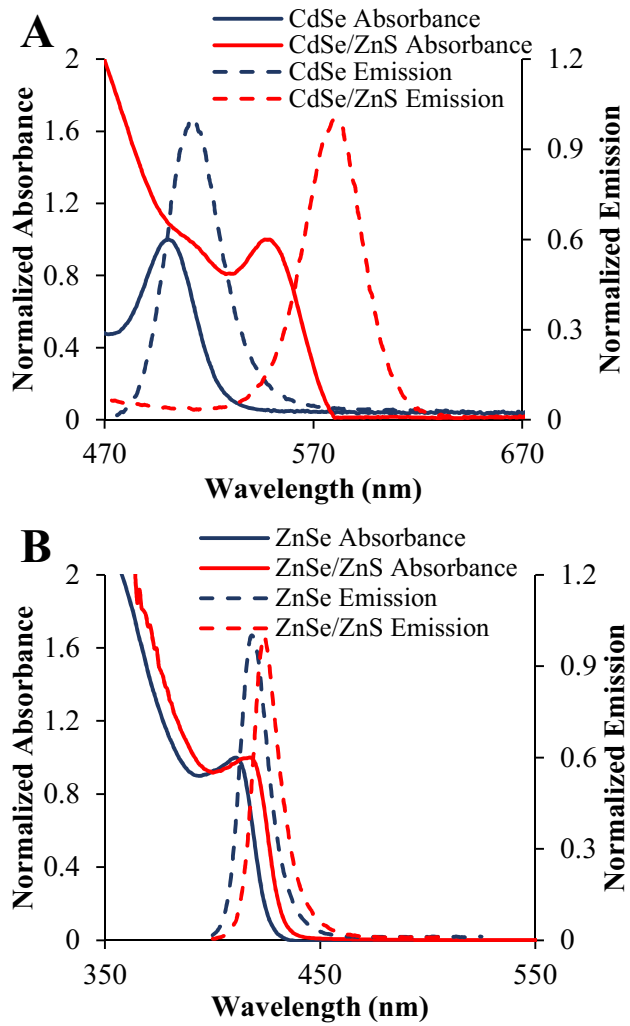
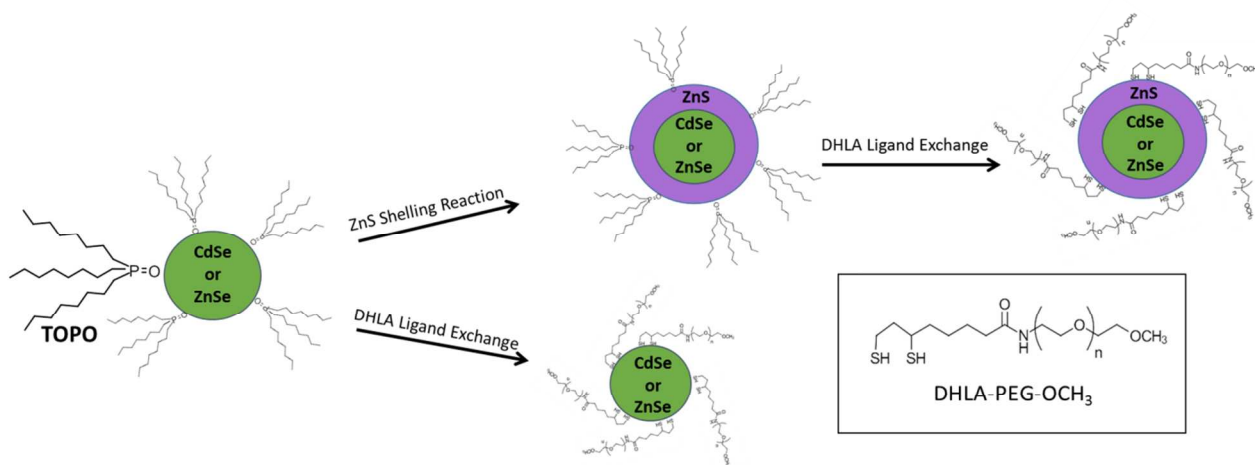


**Figure 1.** Normalized absorbance and emission spectra of CdSe and CdSe/ZnS QD ( $\lambda_{\text{ex}} = 375$  nm) (A), and ZnSe and ZnSe/ZnS QD ( $\lambda_{\text{ex}} = 350$  nm) (B).



**Scheme 1.** Schematic of ZnSe and CdSe QD shelling to form ZnSe/ZnS and CdSe/ZnS QD, and their ligand exchange to enable QD dispersity in aqueous solution by replacing hydrophobic TOPO with DHLA-PEG amphiphilic ligands

1  
2  
3 **Interactions of CdSe and ZnSe QD with Liposomes** - Liposome lysis assays were carried out  
4 to determine the membrane disruption activity of cadmium-containing CdSe and CdSe/ZnS QD,  
5 and cadmium-free ZnSe and ZnSe/ZnS QD. Unlike bacteria or other living organisms,  
6 liposomes do not possess active mechanisms to degrade QD. Therefore, differences in the  
7 interactions between QD and liposomes membranes could only be attributed to differences in  
8 association of the QD with the liposome membrane due to differences in QD size, shape, and  
9 surface chemistry, and to differences in ion dissolution and reactive oxygen species (ROS)  
10 generation that could affect ion interactions with the liposome membrane. It should be noted  
11 that the rates of ROS generation are negligible in our experiments, which are conducted under  
12 room light conditions in the absence of directed QD irradiation. Liposomes, with a phospholipid  
13 composition that models cell membranes of gram negative bacteria, were loaded with 10 mM  
14 calcein. Calcein was chosen as the fluorophore for the liposome lysis assays primarily because  
15 of its high encapsulation efficiency, and the high anti-leaking stability of calcein-containing  
16 liposomes in aqueous solutions.<sup>45</sup> Loading the liposomes with 10 mM calcein resulted in self  
17 quenching of the fluorescent calcein molecules. The calcein-containing liposomes were exposed  
18 to increasing concentrations of cadmium-containing and cadmium-free QD up to 0.5 mg/mL  
19 selenium ion equivalents. The fluorescence of the calcein-containing liposomes was  
20 continuously measured at 515 nm ( $\lambda_{ex} = 480$  nm) during the liposome lysis assays. Membrane  
21 disruption of the liposomes led to the release and dilution of calcein in the sample solutions,  
22 which in turn led to an increase in calcein fluorescence. The QD were selected to have minimal  
23 excitation at 470 nm and minimal fluorescence at 515 nm to minimize spectral overlap with  
24 calcein absorption and fluorescence.  
25  
26  
27  
28  
29  
30  
31  
32  
33  
34  
35  
36  
37  
38  
39  
40

41  
42 Figure 2 describes the liposome lysis efficiency of the cadmium-containing and cadmium-free  
43 QD. Figure 2A and shows the temporal dependence of calcein fluorescence (normalized) of the  
44 calcein-containing liposomes prior to QD exposure (background fluorescence), following the  
45 exposure of the liposomes to CdSe QD (black) and CdSe/ZnS QD (red) which contain 0.5 mg/L  
46 selenium ion equivalents in their core, and following the addition of 1% Triton solution to  
47 disrupt and release all the calcein molecules from the liposomes. The blue curve follows the  
48 fluorescence of calcein-free liposomes when CdSe/ZnS QD with 0.5 mg/L selenium ion  
49 equivalents in their core were added to the solution. The slight increase in fluorescence due to  
50  
51  
52  
53  
54  
55  
56  
57

1  
2  
3 direct excitation of the CdSe/ZnS QD at 470 nm (an unfavorable excitation wavelength)  
4 represents the highest level of optical interference in our QD exposure experiments. The level of  
5 optical interference is significantly lower when CdSe QD within the same concentration range  
6 are added to the calcein-free liposome solutions. The contribution of QD emission due to direct  
7 excitation was therefore neglected based on these control measurements. Figure 2A and 2B  
8 show that all QD types have membrane disruption activity. Figure 2A shows that CdSe/ZnS  
9 QD cause higher liposome lysis compared to non-shelled CdSe QD, which might be attributed  
10 to shell instability. In contrast, Figure 2B shows that ZnSe/ZnS QD cause less liposome lysis  
11 than non-shelled ZnSe QD, indicating a significantly higher ZnS shell stability on ZnSe QD  
12 relative to CdSe QD.  
13  
14  
15  
16  
17  
18  
19

20  
21  
22 The percent liposome lysis efficiency of CdSe and CdSe/ZnS QD (Figure 2C) and ZnSe and  
23 ZnSe/ZnS QD (Figure 2D) was calculated based on the following expression:  
24  
25  
26

27 
$$\% \text{ Lysis} = [(I_{eq} - I_b) / (I_{tri} - I_b)] \times 100 \quad [1]$$
  
28  
29  
30

31 where  $I_{eq}$  is the fluorescence intensity of the liposomes when reaching equilibrium following the  
32 exposure of the calcein-containing liposomes to QD;  $I_b$  is the background fluorescence of the  
33 calcein-containing liposomes prior to QD exposure; and  $I_{tri}$  is the fluorescence intensity of the  
34 liposome sample following complete disruption and release of calcein molecules due to the  
35 exposure of the calcein-containing liposomes to the 1% Triton solution. Figure 2C and 2D show  
36 the concentration dependence of the liposome lysis efficiency when the calcein-containing  
37 liposomes were exposed to increasing concentrations of CdSe QD and CdSe/ZnS QD (Figure  
38 2C), and ZnSe and ZnSe/ZnS QD (Figure 2D). The membrane disruption activity is  
39 concentration-dependent for all QD types. Cadmium-containing CdSe and CdSe/ZnS QD  
40 exhibit higher levels of membrane disruption activity than cadmium-free ZnSe and ZnSe/ZnS  
41 QD. For example, exposure of the calcein-containing liposomes to CdSe and CdSe/ZnS QD  
42 with 0.5 mg/L selenium ion equivalents in their core resulted in  $38 \pm 1\%$  and  $42 \pm 1\%$  liposome  
43 lysis efficiency. In contrast, exposure of the calcein-containing liposomes to ZnSe and  
44 ZnSe/ZnS QD at 10-fold higher selenium ion equivalents in their cores resulted in  $15 \pm 4\%$ , and  
45  $10 \pm 1\%$  liposome lysis efficiency respectively. Coating ZnSe QD with a ZnS shell decreased  
46  
47  
48  
49  
50  
51  
52  
53  
54  
55  
56  
57  
58  
59  
60

their membrane disruption activity almost to the level of liposome lysis observed when the calcein-containing liposomes were exposed to the DHLA-PEG ligands at ppb levels (the levels anticipated if all ligand molecules would be desorbed from the QD surface). In contrast, coating CdSe QD with a ZnS shell slightly increased, rather than decreased, their membrane disruption activity. The differences in lysis efficiency between CdSe and ZnSe QD, and the opposite effect of coating them with a ZnS shell on their membrane disruption activity was unexpected since the synthesis methods used to prepare the CdSe and ZnSe QD and their surface chemistry were nearly identical. The source of this unexpected result is explored in the following paragraphs.

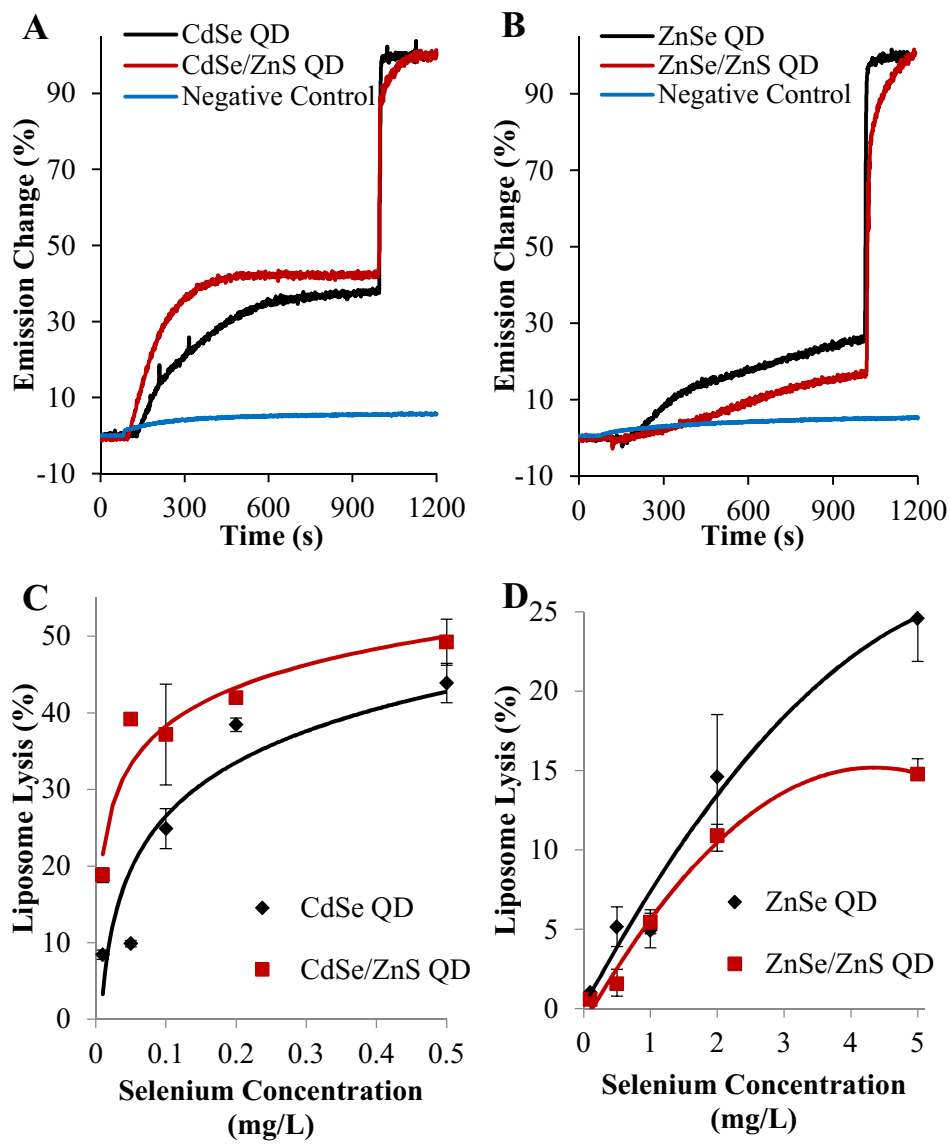


**Figure 2.** Normalized emission traces comparing the membrane disruption activity of CdSe and CdSe/ZnS QD (A), and ZnSe and ZnSe/ZnS QD (B). The negative control (blue) curves follow the exposure of calcein-free liposomes to CdSe/ZnS QD (A) and ZnSe/ZnS QD (B). Figure 2C shows the concentration dependence of the liposome lysis efficiency for CdSe (black) and CdSe/ZnS (red) QD. Figure 2D shows the concentration dependence of the lysis efficiency for ZnSe (black) and ZnSe/ZnS (red) QD. Each liposome lysis efficiency value is the average of three replicate measurements ( $N=3$ ). The error bars are  $\pm$  standard deviation from the mean value.

**Liposomes Lysis Assays of CdSe/ZnS QD with Varying Shell Thickness** - Having observed an increase in membrane disruption activity when CdSe QD are coated with a ZnS shell, we investigated how the shell thickness affects the liposome lysis efficiency of CdSe/ZnS QD. Transmission electron microscopy (TEM) measurements were used to confirm an increase in QD size when CdSe QD were coated with a ZnS shell of increasing thickness (see supportive information for details). Figure 3A shows the temporal dependence of the fluorescence of calcein-containing liposomes prior to QD exposure (background fluorescence), following the exposure to CdSe QD (black), and CdSe/ZnS QD with a shell thickness of one monolayer (green), three monolayers (red), and six monolayers (blue). All experiments were conducted with CdSe and CdSe/ZnS QD that contained 0.5 mg/L in their core as was determined by ICP-MS. Control experiments involving the addition of CdSe and CdSe/ZnS QD of the same concentration to liposome-free and calcein-free liposome solutions showed an instant but negligible increase in QD fluorescence under our illumination conditions ( $\lambda_{\text{ex}} = 480$  nm,  $\lambda_{\text{em}} = 515$  nm). The negligible contribution of QD fluorescence is expected since QD concentrations in our liposome lysis experiments are three orders of magnitude lower than the concentration of calcein in the liposome solution following liposome lysis. The liposome lysis efficiencies were calculated from the curves in Figure 3A using equation 1 (see above) as  $44 \pm 3\%$  for CdSe QD (no shell),  $42 \pm 1\%$  for CdSe/ZnS QD with one monolayer,  $49 \pm 3\%$  for CdSe/ZnS QD with three monolayers, and  $70 \pm 1\%$  CdSe/ZnS QD with six monolayers ZnS shell thickness. A slower membrane disruption efficiency is observed when the liposomes are exposed to CdSe/ZnS QD with one monolayer shell, a shell thickness that seems to delay but not to prevent the liposome lysis. Further increase in shell thickness results in increasing liposome lysis efficiency, most significantly when the CdSe QD are coated with a thick six-monolayer ZnS shell.

ICP-MS measurements of cadmium, zinc, and selenium ions were used to determine the chemical stability of ZnSe QD, ZnSe/ZnS QD, CdSe QD, and CdSe/ZnS QD with varying shell thickness and concentration. Figure 3B describes the results of ICP-MS measurements used to determine the level of ion dissolution in CdSe and CdSe/ZnS QD with varying ZnS shell thickness between one and six monolayers at increasing concentrations from 0 to 0.5 mg/L selenium ion equivalents in QD which were added to a HEPES buffer at pH 7.4. The QD were

1  
2  
3  
4  
5  
6  
7  
8  
9  
10  
11  
12  
13  
14  
15  
16  
17  
18  
19  
20  
21  
22  
23  
24  
25  
26  
27  
28  
29  
30  
31  
32  
33  
34  
35  
36  
37  
38  
39  
40  
41  
42  
43  
44  
45  
46  
47  
48  
49  
50  
51  
52  
53  
54  
55  
56  
57  
58  
59  
60

incubated in HEPES buffer at room temperature for various time intervals ranging from 15 minutes to 24 hours. The QD were then filtered out by passing the QD solution through a 30K MWCO filter under slow speed centrifugation of 2000xg at room temperature. The levels of cadmium and selenium in the supernatant for all QD were negligible. In contrast, CdSe/ZnS QD exhibited significant zinc ion dissolution over 24 hours, which increased with CdSe/ZnS QD concentration and ZnS shell thickness. It should be noted that it is difficult to quantify the amount of released zinc ions from the QD due to high native levels of zinc in aqueous samples and glassware.<sup>46</sup> Nevertheless, the QD concentration dependence and ZnS shell thickness dependence of zinc ions levels in the samples strongly suggest a significant level of zinc ion dissolution, in the mg/L range, from the CdSe/ZnS QD within the time scale of our liposome lysis assays. It is therefore fair to conclude that zinc ion dissolution increases the adverse impact of CdSe/ZnS QD on the liposome membranes beyond their impact due membrane association and disruption. It is important to note that the luminescence properties of the CdSe/ZnS QD, including emission quantum yield and peak width, do not change during the 15-minute long incubation and liposome lysis assays, which were conducted in HEPES buffer at pH 7.4 and room temperature as well. This is consistent with previous studies in our laboratory, which showed that a single monolayer of ZnS shell is sufficient to realize ~90% enhancement in luminescence properties of CdSe/ZnS QD, and the value of additional ZnS shell layers is more in delaying the degradation of the core CdSe QD.<sup>44</sup> It is interesting to note that ZnSe/ZnS QD exhibited significantly higher shell stability, and the levels of zinc ions in the supernatants of incubated ZnSe/ZnS QD were negligible (not shown). This was observed even though CdSe and ZnSe QD were coated with the same ZnS shell using nearly identical shelling conditions. The increased ZnS shell stability on ZnSe QD is attributed to a greater crystal plane matching in ZnSe/ZnS than in CdSe/ZnS QD.

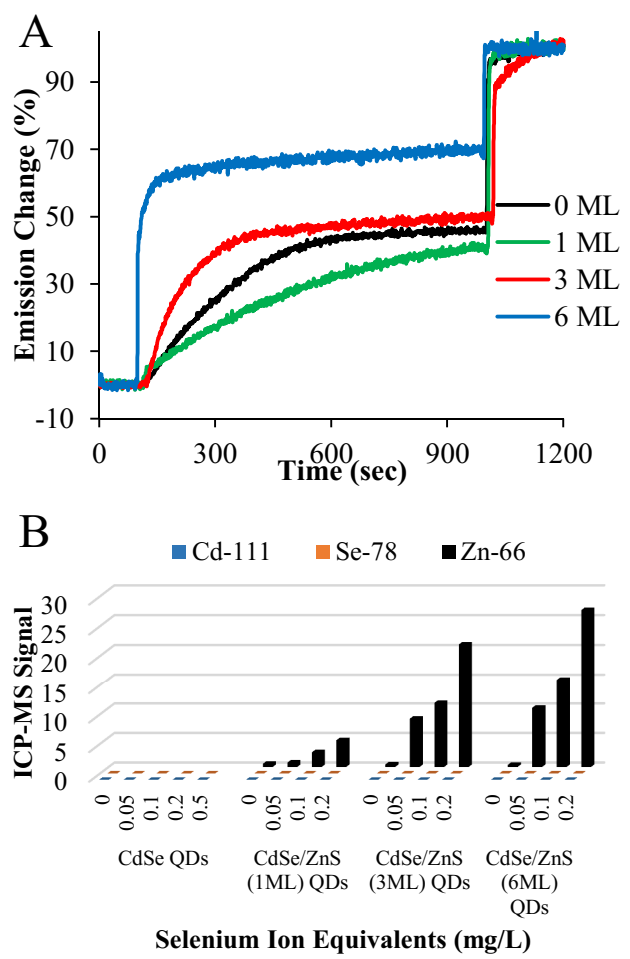


**Figure 3.** Normalized emission traces from calcein-filled liposomes when exposed to CdSe QD with 0 to 6 monolayers (ML) (A). ICP-MS signal intensities of zinc, cadmium, and selenium ions resulting from the dissolution of CdSe QD and CdSe/ZnS QD with one, three and six monolayers shell in HEPES buffer at pH 7.4 (B). Only zinc ion dissolution is observed indicating

degradation of the ZnS shell. N=3 for each condition, and error bars are omitted for clarity.

1  
2  
3 **Association of QD with Liposomes as a Key Contributor to Liposome Membrane**  
4 **Disruption** - The ICP-MS results described above showed negligible cadmium and selenium  
5 ion dissolution from CdSe QD during 15-minute long incubation in liposome free and liposome  
6 containing HEPES buffer solutions at pH 7.4. In addition, ion control experiments revealed a  
7 lack of lysis activity when liposomes were incubated for 15 minutes with QD supernatants (no  
8 QD in the incubation mixture), and in cadmium and selenium ion solutions at concentrations  
9 resulting from total dissolution of CdSe with 0.5 mg/L in their cores. And yet, a measurable  
10 difference between the membrane disruption activity of CdSe and ZnSe QD and an increase in  
11 the membrane disruption activity of CdSe/ZnS QD with increasing shell thickness were  
12 observed. Based on these results we hypothesized that QD association with the liposome  
13 membranes play a major role in the membrane disruption activity of QD and that the association  
14 of QD with liposomes differs for different QD types. Association between the QD and the  
15 liposome destabilizes the liposome membranes mechanically. The instability of ZnS shell on  
16 CdSe/ZnS QD results in zinc ion dissolution when the QD degrade, and the increase in local ion  
17 concentration near the membrane could also contribute to membrane disruption. To validate this  
18 hypothesis, we prepared NBD-labeled liposomes and investigated their interactions with CdSe  
19 and ZnSe QD. NBD is an environmentally sensitive dye. In the literature, a fluorescence  
20 increase and a fluorescence lifetime decrease were reported with decreasing polarity of the  
21 NBD environment.<sup>42</sup> In contrast, a fluorescence decrease was reported when NBD molecules  
22 react with ROS.<sup>41</sup> Fluorescence spectra of NBD prior to and following exposure of NBD  
23 liposomes to CdSe and ZnSe QD are shown in Figures 4A and 4B. The fluorescence spectra of  
24 NBD liposomes ( $\lambda_{\text{ex}} = 470\text{nm}$  and  $\lambda_{\text{em max}} = 515\text{nm}$ ) prior to and following QD exposure are  
25 shown in black and red, respectively. The residual fluorescence spectra of CdSe and ZnSe QD  
26 at this unfavorable excitation wavelength are shown in blue. A 6-fold increase in the  
27 fluorescence intensity of the NBD liposomes is observed following their exposure to CdSe  
28 (Figure 4A) and ZnSe (Figure 4B) QD. This is attributed to decreased polarity of the NBD  
29 environment due to the associating of the PEG-coated QD with the liposome membranes, which  
30 effectively shield the NBD headgroup from water molecules and ions in the buffer solution. The  
31 lack of fluorescence decrease following the incubation of QD with the liposomes strongly  
32 suggests that ROS are not formed and therefore not a significant contributor to membrane  
33 disruption under our experimental conditions (short exposure, no UV irradiation). Fluorescence  
34  
35  
36  
37  
38  
39  
40  
41  
42  
43  
44  
45  
46  
47  
48  
49  
50  
51  
52  
53  
54  
55  
56  
57  
58  
59  
60

1  
2  
3 lifetime measurements shown in Figure 4C for CdSe and 4D for ZnSe QD provide additional  
4 indication that the QD associate with the liposome membranes. Table 1 summarizes the  
5 fluorescence lifetime and the exponential terms used to fit the fluorescence lifetime decay  
6 curves of NBD liposomes prior and following a 4-hour long exposure to CdSe and ZnSe QD. A  
7 decrease in the fluorescence lifetime from  $5.87 \pm 0.23$  nsec to  $5.17 \pm 0.03$  nsec and to  $5.23 \pm$   
8  $0.03$  nsec when the NBD liposomes are incubated for 4 hours with CdSe and ZnSe QD,  
9 respectively, is observed. Additionally, the fluorescence lifetime decay curve of NBD liposomes  
10 prior to QD exposure, is described by two exponential terms with  $\tau_1 = 2.81$  nsec and  $\tau_2 = 9.58$   
11 nsec with almost equal weights of ~55 and 45%. These two terms are attributed to the NBD  
12 heterogeneous environment, which is equally affected by the hydrophobic backbone of the  
13 liposome membrane and the outer aqueous environment of the liposomes. A significantly  
14 increased mono-exponential character is observed when the PEG-coated QD interact with the  
15 liposome membrane. The fluorescence lifetime decay curves (red) are still described by two  
16 exponential terms, for CdSe QD  $\tau_1 = 3.78$  nsec and  $\tau_2 = 9.24$  nsec and for ZnSe QD  $\tau_1 = 3.84$   
17 nsec and  $\tau_2 = 9.43$  nsec, but their weights change to ~72 and 28% in both QD types. The  
18 decrease in fluorescence lifetime and the increase in mono-exponential character of the  
19 fluorescence lifetime decay curves are consistent with a decrease in the polarity of the NBD  
20 environment, which is attributed to association of the PEG-coated QD to the NBD liposomes.  
21 As expected, the change in NBD fluorescence and fluorescence lifetime does not depend on the  
22 QD core composition. It only depends on the surface chemistry of the QD, which is nearly  
23 identical for CdSe and ZnSe QD as both QD types undergo a ligand exchange process to replace  
24 TOPO with DHLA-PEG molecules to enable aqueous miscibility of the QD. Association of the  
25 QD with the liposome membranes is critical to their membrane disruption activity, which  
26 depends on their dissolution rate following their association with the liposome membranes.  
27  
28  
29  
30  
31  
32  
33  
34  
35  
36  
37  
38  
39  
40  
41  
42  
43  
44  
45  
46  
47  
48  
49  
50  
51  
52  
53  
54  
55  
56  
57  
58  
59

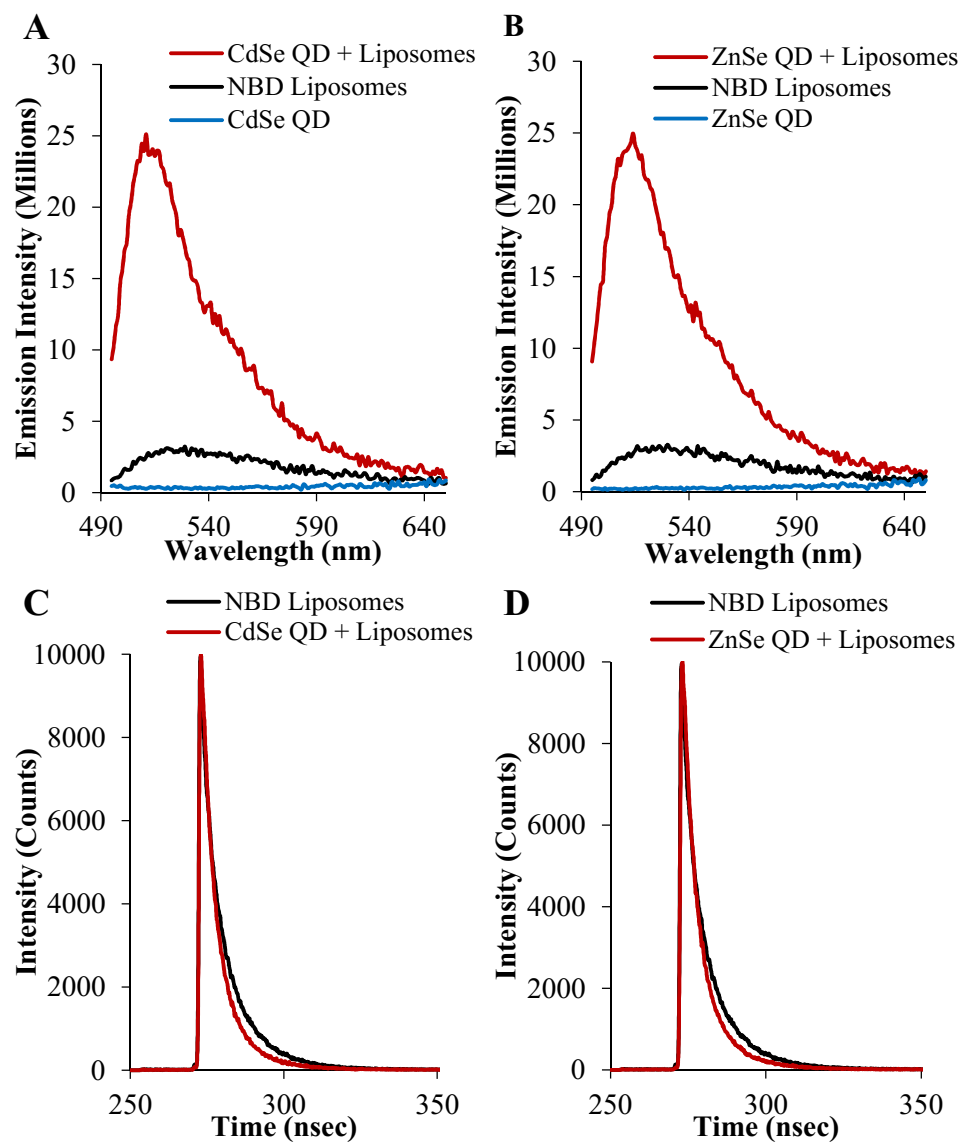


**Figure 4.** The fluorescence intensity of NBD-labeled liposomes (black), QD (blue), and following a 4-hour incubation of NBD-labeled liposomes with QD (red) show significant NBD fluorescence increase for both CdSe (A) and ZnSe (B) QD ( $\lambda_{\text{ex}} = 470\text{nm}$ ). Time resolved photoluminescence decay curves of NBD-liposomes (black) and following a 4-hour incubation with QD (red) for CdSe QD (C) and ZnSe QD (D) show a decrease in fluorescence lifetime ( $\lambda_{\text{ex}} = 470\text{nm}$ ,  $\lambda_{\text{em}} = 515\text{nm}$ ).

	weighted fluorescence lifetime $\tau$ (nsec)	$\tau_1$ (nsec)	$A_1$ (%)	$\tau_2$ (nsec)	$A_2$ (%)
NBD- Liposomes	$5.87 \pm 0.23$	2.81	54.81	9.58	45.17
CdSe QD and Liposomes	$5.23 \pm 0.02$	3.78	72.51	9.24	27.49
ZnSe QD and Liposomes	$5.17 \pm 0.03$	3.84	72.48	9.43	27.52

**Table 1.** A summary of the fluorescence lifetime and exponential terms used to fit the fluorescence lifetime decay curves for NBD liposomes prior to and following exposure to CdSe and ZnSe QD. The decrease in fluorescence lifetime decrease, and the change from a bi-exponential to a mono-exponential character of the fluorescence lifetime decay curves are consistent with QD association with the liposome membranes.

1  
2  
3 **The Impact of Cadmium-Free and Cadmium-Containing QD on *Shewanella Oneidensis***  
4  
5 **MR-1 Bacteria.** The liposome lysis assays showed membrane disruption activity of all QD  
6 types, which is attributed to QD-membrane association that leads to membrane disruption. In  
7 our liposome experiments, CdSe and CdSe/ZnS QD showed higher membrane disruption  
8 activity than ZnSe and ZnSe/ZnS QD. We hypothesized that the interactions between the QD  
9 and negatively charged bacterial membranes would be similar to the interactions of QD with  
10 negatively charged liposomes. To test this hypothesis, we investigated the interactions between  
11 cadmium-free, ZnSe and ZnSe/ZnS QD, and cadmium-containing CdSe and CdSe/ZnS QD, and  
12 *Shewanella oneidensis* MR-1 bacteria. *Shewanella oneidensis* was chosen for the study because  
13 it is an environmentally relevant bacteria, which was previously used in similar nanoparticle  
14 exposure studies.<sup>31, 32</sup> We utilized TEM, ICP-MS, and hyperspectral imaging measurements to  
15 investigate the interactions between QD and bacterial cells, and then measured the impact of  
16 QD exposure on bacterial cell viability.

17  
18  
19  
20  
21  
22  
23  
24  
25  
26  
27 TEM measurements provide qualitative assessment of the interactions between QD and  
28 bacteria. Representative TEM images of bacterial cells which were exposed to 1 mg/L  
29 CdSe/ZnS QD (the most disruptive QD to liposomes and bacterial cells) are shown in Figure 5.  
30 The low magnification required to view the bacteria (scale bars of 0.2 to 1  $\mu$ m) enables the  
31 observation of dark spots, possibly of QD aggregates associated with the cells but not individual  
32 QD which are only  $\sim$ 5nm in diameter. Images A and B show distorted cells with the release of  
33 cell organelles as well as disintegrated cell membranes. Dark spots, possibly of QD aggregates,  
34 are seen on or near cells in the TEM images. The images reveal a significant damage to the cells  
35 due to the interaction with the QD, which is consistent with our QD-liposome lysis assays.

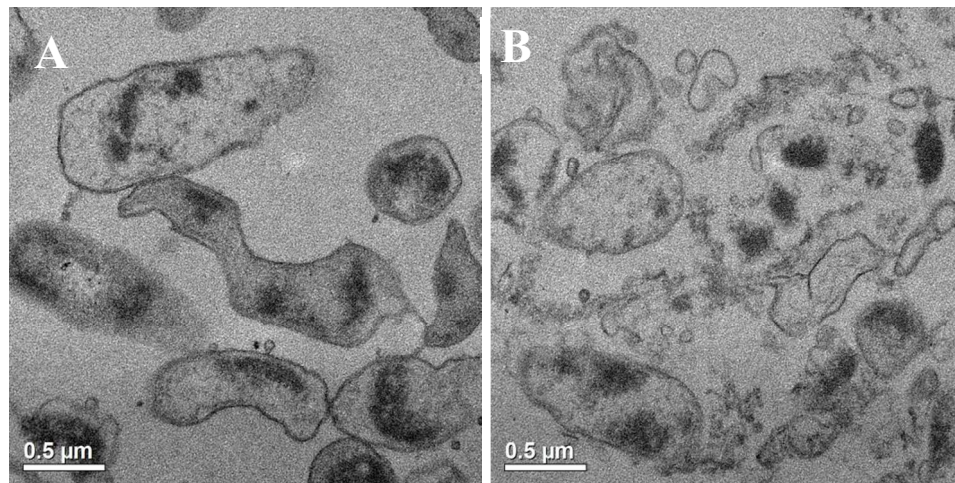


**Figure 5.** Representative biological TEM micrographs of *Shewanella oneidensis* MR-1 bacteria samples treated with CdSe/ZnS QD. Image A shows association of CdSe/ZnS QD with bacteria and cell malformation. Image B shows significant disintegration of bacterial cells due to interactions with CdSe/ZnS QD.

1  
2  
3 ICP-MS experiments of washed bacterial samples digested following their incubation with  
4 ZnSe, ZnSe/ZnS, CdSe, and CdSe/ZnS QD were used to determine the level of association of  
5 these QD with *Shewanella oneidensis* MR-1 cells. Control measurements of digested pellets of  
6 *Shewanella oneidensis* in the absence of QD show no detectable zinc or cadmium ions.  
7 Digested pellets of bacteria that were incubated with 0.5 to 5 mg/L QD in HEPES buffer  
8 solutions at pH 7.4 show levels of cadmium (cadmium containing QD) and zinc (cadmium-free  
9 QD) that were significantly higher than the levels of these ions in control QD samples in the  
10 absence of bacteria. For example, the washing of 2 mg/L CdSe/ZnS QD control (no bacteria)  
11 had a measured cadmium level of 27  $\mu$ g/L. In contrast, when bacterial cells were exposed to 2  
12 mg/L CdSe/ZnS QD the level of cadmium pelleted with the bacteria was about 10-fold higher at  
13 200  $\mu$ g/L. Interestingly, the level of cadmium and zinc in QD-bacterial samples, which were  
14 exposed to CdSe/ZnS and ZnSe/ZnS QD was 3-fold higher than the level of cadmium and zinc  
15 in QD-bacterial samples which were exposed to CdSe and ZnSe core QD. The higher affinity  
16 of CdSe/ZnS QD than the affinity of CdSe QD to bacterial cells is consistent with the liposome  
17 assays described earlier, but the higher affinity of ZnSe/ZnS QD than ZnSe QD to bacterial cells  
18 is not. This shows the limitations of the using simple liposomes to model complex bacteria. The  
19 higher levels of cadmium and zinc in QD-incubated bacteria provide additional evidence for  
20 QD-bacteria association.  
21  
22  
23  
24  
25  
26  
27  
28  
29  
30  
31  
32  
33

1  
2  
3 Hyperspectral dark field microscopy was also used to study the interactions between QD and  
4 bacterial cells. This technique provides the capability to identify and locate objects, for example  
5 nanoparticles and cells as long as they show unique optical reflectance signature.<sup>47</sup> The method  
6 is somewhat limited in the ability to locate nanoparticles in the field because it is diffraction  
7 limited but still able to indicate colocalization of the nanoparticles with the much larger  
8 bacterial cells. The hyperspectral data cube acquisition, namely hyperspectral “pushbroom”  
9 scanning, generates 3D data consist of two spatial (x,y) and one spectral (z) dimensions.<sup>48</sup>  
10 Hence, a hyperspectral image can be treated as a dark field image with the spectral information  
11 associated with each pixel of the image.<sup>49</sup> The work flow includes dark field imaging,  
12 hyperspectral data acquisition, spectral library construction, spectral library filtering, and  
13 finally, QD and bacterial cell mapping. Figure 6 exhibits the hyperspectral images (left column)  
14 of *Shewanella oneidensis* (named *S. Oneidensis* in the figure), CdSe QD, and CdSe/ZnS QD,  
15 and corresponding spectral libraries (right column) obtained by the region-of-interest (ROI) tool  
16 that converts selected pixels into spectral libraries for subsequent QD and bacterial cell mapping  
17 in QD-incubated bacterial samples. Specifically, 499 pixels were collected to build the  
18 *Shewanella oneidensis* library, 438 pixels to build the CdSe QD library, and 403 pixels to build  
19 the CdSe/ZnS QD library. Maximum (max), minimum (min), and mean reflectance intensity are  
20 described in libraries files, along with standard deviation ( $\pm$ Stdev), from which it can be  
21 qualitatively determined that the average reflectance intensity of bacteria is much lower than  
22 those of QD. In addition, spectral library function anchored with CytoViva software was  
23 performed to cross-compare the libraries of bacteria and QD. It turned out that there was no  
24 library filtered out for both cases, indicating the uniqueness of their spectral files. Moreover,  
25 QD libraries were loaded into the spectral angle mapper (SAM) function to map the location of  
26 QD in the hyperspectral images of CdSe and CdSe/ZnS QD. The SAM function provides a  
27 convenient and automated mapping method, of which the algorithm differentiates the spectral  
28 libraries and provides information about the location and analogy of endmember pixels in an  
29 input image.<sup>49, 50</sup> This information allows us to map precise QD location and false-colored them  
30 red. For the next step, the presence of QD co-localized with *Shewanella oneidensis* cells after  
31 exposure was investigated using hyperspectral microscopy, as displayed by Figure 7. The pixels  
32 representing QD are pseudo-colored with red. In both exposure samples, it is observable that  
33 there is proximity between QD and bacteria cells. The proximity, and in many cases overlap,  
34

1  
2  
3 between the spectral signatures for bacterial cells and QD support our conclusion from the  
4 liposome assays that the QD associate with the negatively charged membranes. This in turn  
5 leads to a high local ion concentration as the QD dissolve. The increase in local ion  
6 concentration leads to membrane disruption. As a caveat, the diffraction limit binds this  
7 imaging technique, so even overlap of spectral signatures does not guarantee direct physical  
8 contact between the micron-scale bacteria (which can be resolved) and the nanoscale QD  
9 (which cannot be resolved).  
10  
11  
12  
13  
14  
15  
16  
17  
18  
19  
20  
21  
22  
23  
24  
25  
26  
27  
28  
29  
30  
31  
32  
33  
34  
35  
36  
37  
38  
39  
40  
41  
42  
43  
44  
45  
46  
47  
48  
49  
50  
51  
52  
53  
54  
55  
56  
57  
58  
59  
60

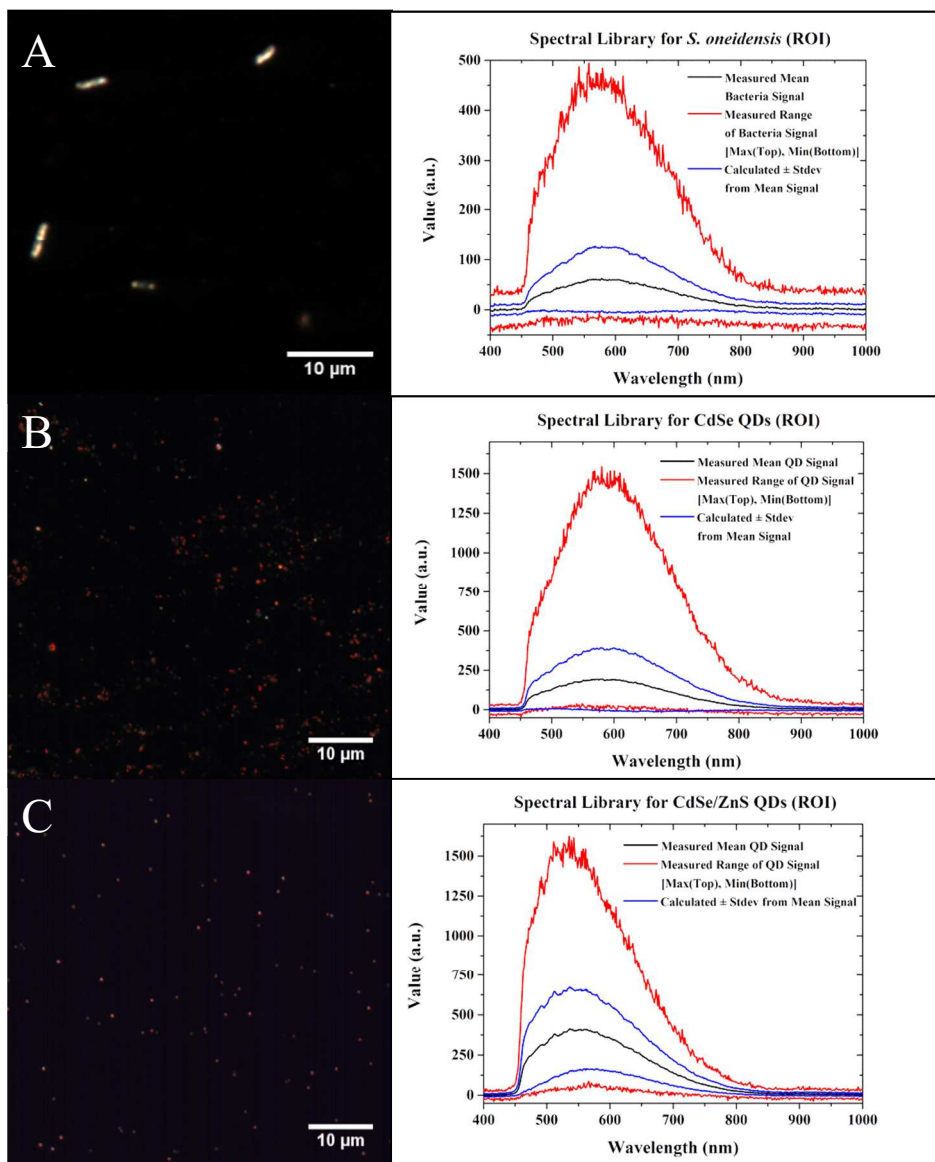


**Figure 6.** Hyperspectral reflectance microscopy images of *Shewanella oneidensis* MR-1 (A), CdSe QD (B), and CdSe/ZnS (3ML) QD (C), with the QD false-colored red. The minimum, maximum, and median reflectance spectra for each sample are captured to build a spectral reference library which is shown to the right of each image. The libraries enable identification of bacterial cells and QD in mixed samples.

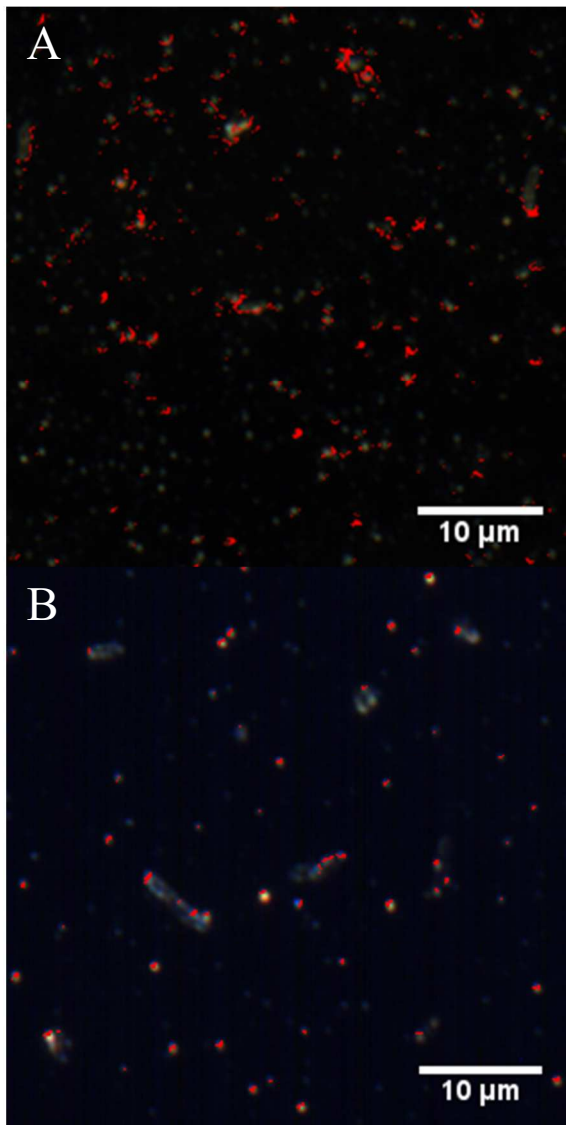


**Figure 7.** Images of QD-incubated bacteria samples analyzed using the reference spectral libraries of *Shewanella oneidensis* (gray) exposed to CdSe QD (A) or CdSe/ZnS (3 ML) (B). In both images, pixels displaying the QD spectral signatures are colored red. In many cases, QD are at the vicinity or overlap with bacterial cells,

which is indicative of QD membrane association.

1  
2  
3 Realizing the important role of membrane association on the interactions between QD and  
4 liposome, we conducted bacterial viability assays to see if the apparent liposome-QD  
5 association and the likely association between bacteria-QD indicated by TEM, ICP-MS, and  
6 hyperspectral imaging would lead to dose-dependent impact of QD on *Shewanella oneidensis*  
7 MR-1.  
8  
9

10  
11  
12 Bacterial cell cultures were exposed to ZnSe, ZnSe/ZnS, CdSe, or CdSe/ZnS QD at  
13 concentrations ranging from 0.01 to 0.5 mg/L selenium equivalents in the QD cores. Figure 8A  
14 shows bacterial cell cultures following exposure to increasing concentrations ranging from 0 to  
15 0.5 mg/L of ZnSe (left) and CdSe (right) QD. Exposure of *Shewanella oneidensis* MR-1 to  
16 ZnSe QD had negligible impact on their viability even at the highest concentration of 0.5 mg/L  
17 selenium equivalents. Similarly, ZnSe/ZnS QD exposure did not impact bacterial cell viability  
18 (Figure SI-5). In contrast, exposure of *Shewanella oneidensis* MR-1 cells to CdSe QD at 0.01  
19 mg/L selenium equivalents led to almost total reduction in *Shewanella oneidensis* viability. In  
20 agreement with the liposome assays, an even greater effect was observed when the bacterial  
21 cells were exposed to similar levels of CdSe/ZnS QD. To evaluate the relevance of the liposome  
22 assays as a model for the bacterial response to QD exposure, we also investigated the impact of  
23 CdSe/ZnS QD with varying shell thickness on the viability of *Shewanella oneidensis* MR-1.  
24 Figure 8B describes the bacterial cell viability (%) as a function of CdSe/ZnS QD concentration  
25 (selenium equivalents) for CdSe QD (black) and CdSe/ZnS QD with shell thickness of one  
26 monolayer (green), three monolayers (red), and six monolayers (red). A concentration-  
27 dependent decrease in bacterial viability is shown for all cadmium-based QD, and a greater  
28 decrease in bacterial viability is observed for CdSe/ZnS QD with increasing ZnS shell  
29 thickness. These results are indicative of the complex nature of the interactions between  
30 luminescent QD and bacteria. On one hand, passivating CdSe QD with a higher energy bandgap  
31 shell of ZnS is known to decrease the rate of ROS generation when irradiated and lower their  
32 toxicity.<sup>15, 20-22</sup> On the other hand, the chemical instability of the shell due to crystal plane  
33 mismatches along the core/shell interface<sup>51, 52</sup>, particularly in complex aqueous solutions,  
34 increases their rate of zinc ion dissolution, and increases QD toxicity against the *Shewanella*  
35 *oneidensis* MR-1 bacteria.  
36  
37  
38  
39  
40  
41  
42  
43  
44  
45  
46  
47  
48  
49  
50  
51  
52  
53  
54  
55  
56  
57  
58  
59  
60

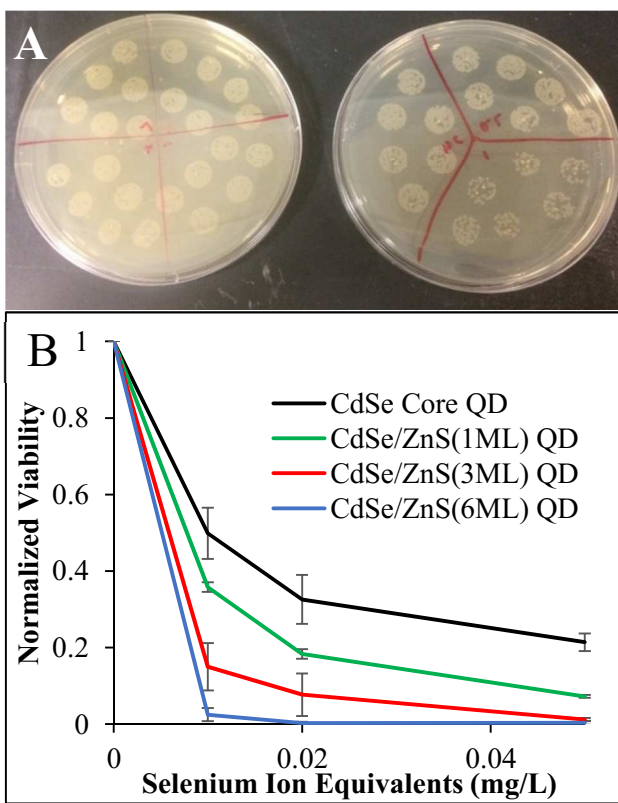


**Figure 8.** *Shewanella oneidensis* MR-1 colony growth after exposure to increasing concentrations of ZnSe QD (left) and CdSe QD (right) compared to negative controls (NC) on each plate (A). Exposing the cells to ZnSe/ZnS QD does not impact cell viability (Figure SI-5). In contrast, a significant reduction in viability is seen in *Shewanella oneidensis* viability results after exposure to CdSe/ZnS QD. Normalized bacterial cell viability as a function of ZnS shell thickness in CdSe/ZnS QD (B). Increasing the QD shell thickness decreases

cell viability in a concentration dependent manner. N=4 biological replicates for each condition, and the error bars represent standard deviation among those replicates.

## SUMMARY AND CONCLUSIONS

This study assessed the interactions between cadmium-containing and cadmium-free luminescent QD with negatively charged liposomes, which are often used to model gram negative bacteria, and *Shewanella oneidensis* MR-1, an environmentally relevant gram-negative bacteria. Fluorescence lysis assays of calcein-containing liposomes show that all QD types interact with the liposomes, but the level of interactions is higher for cadmium-containing QD, especially CdSe/ZnS QD. The results suggest that association of the QD with the liposome membrane leads to membrane disruption, which is mechanical in nature and depends on the QD concentration and their affinity to the liposome membranes. The short time scale of the liposome lysis assays precludes ion dissolution of free QD (not associated with the membrane) as a main contributor to liposome lysis. Additionally, since the liposomes are only irradiated with room light, the observed membrane disruption cannot be attributed to ROS generation. BioTEM, ICP-MS and hyperspectral imaging measurements suggest that the QD also associate with the negatively-charged membranes of *Shewanella oneidensis* MR-1 bacterial cells. As expected, cadmium-free ZnSe and ZnSe/ZnS QD minimally impact on the viability of *Shewanella oneidensis* MR-1. In contrast, a short exposure time, as short as only 15 minutes, of CdSe or CdSe/ZnS QD to bacterial cells results in a significant reduction in bacterial cell viability. Ion control experiments show that when CdSe or CdSe/ZnS QD are completely dissolved in solution, the resulting ion levels are not sufficient to induce a devastating impact on the cells, and yet exposure of the cells to QD does. The QD impact on liposomes and bacterial cells in this study is attributed to strong association between the QD and liposomes or bacterial cells, which does not cease after the cells are separated from unbound QD to end the exposure. Surprisingly, the impact of shelling CdSe QD with a ZnS shell, which is done to enhance the QD emission properties, to minimize ROS generation, and to prevent direct contact between the toxic cadmium-containing cores and the liposomes or bacterial membrane, increases rather than decreases, membrane disruption in both the liposomes and bacterial cultures. These are unwelcome findings since it is generally accepted that shelling cadmium core QD with a ZnS shell would lower QD toxicity due to a reduced rate of ROS generation. The increased membrane disruption of CdSe/ZnS QD compared to CdSe QD and with increasing shell thickness could be attributed to increased affinity and association between CdSe/ZnS and

1  
2  
3 liposomes and bacterial cells. It is also possible that crystal plane mismatches between the core  
4 CdSe QD and the ZnS shell leads to inherent chemical instability of CdSe/ZnS QD<sup>51, 52</sup>, and in  
5 turn to a high rate of zinc ion dissolution from the QD. The dissolution of the ZnS following  
6 association of the CdSe/ZnS QD further destabilize the membrane. The high local concentration  
7 of zinc ions near the membrane could also enhance membrane disruption of the liposomes and  
8 bacterial cells.  
9  
10  
11  
12

## 13 ASSOCIATED CONTENT

### 14 Supporting Information

15 TEM of QD, time resolved photoluminescence measurements of QD, DLS measurements of  
16 liposomes exposed to zinc and cadmium ion controls, viability results for bacteria exposed to  
17 ZnSe and ZnSe/ZnS QD.  
18  
19  
20  
21  
22  
23

## 24 AUTHOR INFORMATION

### 25 Corresponding Author

26 \*Email: zrosenzw@umbc.edu.

### 27 ORCID

28 Denise N. Williams: 0000-0002-6314-2052

29 Sunipa Pramanik: 0000-0001-6450-2593

30 Richard P. Brown: 0000-0001-5145-5425

31 Bo Zhi: 0000-0002-1918-5012

32 Eileen McIntire: 0000-0001-8034-7087

33 Natalie V. Hudson-Smith: 0000-0002-2642-0711

34 Christy L. Haynes: 0000-0002-5420-5867

35 Zeev Rosenzweig: 0000-0001-6098-3932

### 36 Author Contributions

37 The manuscript was written through contributions of all authors. All authors have given  
38 approval to the final version of the manuscript.  
39  
40  
41  
42  
43  
44  
45  
46  
47  
48  
49  
50  
51  
52

## 53 ACKNOWLEDGEMENTS

1  
2  
3 Work investigating liposome and bacterial response to quantum dots was supported by the  
4 National Science Foundation Center for Chemical Innovation (CCI) program Award CHE-  
5 1503408 for the Center for Sustainable Nanotechnology. Work involving bacterial TEM  
6 characterization was carried out in the Characterization Facility at the University of Minnesota,  
7 which receives partial support from the MRSEC program (DMR-1420013). Denise N.  
8 Williams' quantum dot syntheses were supported by the National Science Foundation Award  
9 CHE-1506995, including an NSF AGEP graduate fellowship award under CHE-1506995.  
10 Supplemental fellowship support to Denise N. Williams and Richard P. Brown was provided by  
11 the National Institute of Health Training Grant NIH-T32-GM066706. The authors thank Dr.  
12 Alline Myers of the National Institute for Standards and Technology (NIST) Center for  
13 Nanoscale Science and Technology for assistance with HRTEM imaging and Fang Zhou at the  
14 University of Minnesota for microtoming BioTEM samples.  
15  
16  
17  
18  
19  
20  
21  
22  
23  
24  
25  
26  
27  
28  
29  
30  
31  
32  
33  
34  
35  
36  
37  
38  
39  
40  
41  
42  
43  
44  
45  
46  
47  
48  
49  
50  
51  
52  
53  
54  
55  
56  
57  
58  
59  
60

1  
2  
3  
4  
5  
6  
7  
8  
9  
10  
11  
12  
13  
14  
15  
16  
17  
18  
19  
20  
21  
22  
23  
24  
25  
26  
27  
28  
29  
30  
31  
32  
33  
34  
35  
36  
37  
38  
39  
40  
41  
42  
43  
44  
45  
46  
47  
48  
49  
50  
51  
52  
53  
54  
55  
56  
57  
58  
59  
60  

## REFERENCES

1. Kamat, P.; Scholes, G., Quantum Dots Continue to Shine Brightly. *J. Phys. Chem. Lett.* 2016, 7, 584-585.
2. Liang, X.; Grice, J.; Zhu, Y.; Liu, D.; Sanchez, W.; Li, Z.; Crawford, D.; Le Couteur, D.; Cogger, V.; Liu, X.; Xu, Z.; Roberts, M., Intravital Multiphoton Imaging of the Selective Uptake of Water-Dispersible Quantum Dots into Sinusoidal Liver Cells. *Small* 2015, 11, 1711-1720.
3. Xu, G.; Zeng, S.; Zhang, B.; Swihart, M.; Yong, K.; Prasad, P., New Generation Cadmium-Free Quantum Dots for Biophotonics and Nanomedicine. *Chem. Rev.* 2016, 116, 12234-12327.
4. Bimberg, D., Quantum Dots for Lasers, Amplifiers and Computing. *J. Phys. D: Appl. Phys.* 2005, 38, 2055-2058.
5. Zhao, K.; Pan, Z.; Zhong, X., Charge Recombination Control for High Efficiency Quantum Dot Sensitized Solar Cells. *J. Phys. Chem. Lett.* 2016, 7, 406-417.
6. Bang, J.; Park, J.; Lee, J.; Won, N.; Nam, J.; Lim, J.; Chang, B.; Lee, H.; Chon, B.; Shin, J.; Park, J.; Choi, J.; Cho, K.; Park, S.; Joo, T.; Kim, S., ZnTe/ZnSe (Core/Shell) Type-II Quantum Dots: Their Optical and Photovoltaic Properties. *Chem. Mater.* 2010, 22, 233-240.
7. Ji, W.; Jing, P.; Xu, W.; Yuan, X.; Wang, Y.; Zhao, J.; Jen, A., High Color Purity ZnSe/ZnS Core/Shell Quantum Dot Based Blue Light Emitting Diodes with an Inverted Device Structure. *Appl. Phys. Lett.* 2013, 103.
8. Vasudevan, D.; Gaddam, R.; Trinchi, A.; Cole, I., Core-Shell Quantum Dots: Properties and Applications. *J. Alloys Compd.* 2015, 636, 395-404.
9. Reiss, P.; Protiere, M.; Li, L., Core/Shell Semiconductor Nanocrystals. *Small* 2009, 5, 154-168.
10. Protesescu, L.; Yakunin, S.; Bodnarchuk, M.; Krieg, F.; Caputo, R.; Hendon, C.; Yang, R.; Walsh, A.; Kovalenko, M., Nanocrystals of Cesium Lead Halide Perovskites (CsPbX<sub>3</sub>, X = Cl, Br, and I): Novel Optoelectronic Materials Showing Bright Emission with Wide Color Gamut. *Nano Lett.* 2015, 15, 3692-3696.

1  
2  
3 11. Liu, W.; Zhang, Y.; Ruan, C.; Wang, D.; Zhang, T.; Feng, Y.; Gao, W.; Yin, J.; Wang,  
4 Y.; Riley, A.; Hu, M.; Yu, W., ZnCuInS/ZnSe/ZnS Quantum Dot-Based Downconversion  
5 Light-Emitting Diodes and Their Thermal Effect. *J. Nanomater.* 2015.  
6  
7 12. Fu, P.; Xia, Q.; Hwang, H.; Ray, P.; Yu, H., Mechanisms of Nanotoxicity: Generation of  
8 Reactive Oxygen Species. *J. Food Drug Anal.* 2014, 22, 64-75.  
9  
10 13. Drobintseva, A. O.; Matyushkin, L. B.; Aleksandrova, O. A.; Drobintsev, P. D.;  
11 Kvetnoy, I. M.; Mazing, D. S.; Moshnikov, V. A.; Polyakova, V. O.; Musikhin, S. F.,  
12 Colloidal CdSe and ZnSe/Mn Quantum Dots: Their Cytotoxicity and Effects on Cell  
13 Morphology. *St. Petersburg Polytechnical University Journal: Physics and Mathematics*  
14 2015, 1, 272-277.  
15  
16 14. Ippen, C.; Greco, T.; Kim, Y.; Kim, J.; Oh, M.; Han, C.; Wedel, A., ZnSe/ZnS Quantum  
17 Dots as Emitting Material in Blue QD-LEDs with Narrow Emission Peak and Wavelength  
18 Tunability. *Org. Electron.* 2014, 15, 126-131.  
19  
20 15. Xie, R.; Battaglia, D.; Peng, X., Colloidal InP Nanocrystals as Efficient Emitters Covering  
21 Blue to Near-Infrared. *J. Am. Chem. Soc.* 2007, 129, 15432-+.  
22  
23 16. Zhao, Y.; Liu, Q.; Shakoor, S.; Gong, J.; Wang, D., Transgenerational Safety of  
24 Nitrogen-doped Graphene Quantum Dots and the Underlying Cellular Mechanism in  
25 *Caenorhabditis elegans*. *Toxicology Research* 2015, 4, 270-280.  
26  
27 17. Erogbogbo, F.; Yong, K.; Roy, I.; Xu, G.; Prasad, P.; Swihart, M., Biocompatible  
28 Luminescent Silicon Quantum Dots for Imaging of Cancer Cells. *Acs Nano* 2008, 2, 873-  
29 878.  
30  
31 18. Das, A.; Snee, P., Synthetic Developments of Nontoxic Quantum Dots. *Chemphyschem*  
32 2016, 17, 598-617.  
33  
34 19. Maurer-Jones, M.; Gunsolus, I.; Murphy, C.; Haynes, C., Toxicity of Engineered  
35 Nanoparticles in the Environment. *Anal. Chem.* 2013, 85, 3036-3049.  
36  
37 20. Priester, J.; Stoimenov, P.; Mielke, R.; Webb, S.; Ehrhardt, C.; Zhang, J.; Stucky, G.;  
38 Holden, P., Effects of Soluble Cadmium Salts Versus CdSe Quantum Dots on the Growth  
39 of Planktonic *Pseudomonas aeruginosa*. *Environ. Sci. Technol.* 2009, 43, 2589-2594.  
40  
41 21. Derfus, A.; Chan, W.; Bhatia, S., Probing the Cytotoxicity of Semiconductor Quantum  
42 Dots. *Nano Lett.* 2004, 4, 11-18.  
43  
44  
45  
46  
47  
48  
49  
50  
51  
52  
53  
54  
55  
56  
57  
58  
59  
60

1  
2  
3 22. Lai, L.; Li, S.; Feng, J.; Mei, P.; Ren, Z.; Chang, Y.; Liu, Y., Effects of Surface Charges  
4 on the Bactericide Activity of CdTe/ZnS Quantum Dots: A Cell Membrane Disruption  
5 Perspective. *Langmuir* 2017, 33, 2378-2386.  
6  
7 23. Lu, Z.; Li, C.; Bao, H.; Qiao, Y.; Toh, Y.; Yang, X., Mechanism of Antimicrobial  
8 Activity of CdTe Quantum Dots. *Langmuir* 2008, 24, 5445-5452.  
9  
10 24. Green, M.; Howman, E., Semiconductor Quantum Dots and Free Radical Induced DNA  
11 Nicking. *Chem. Comm.* 2005, 0, 121-123.  
12  
13 25. Manshian, B.; Soenen, S.; Al-Ali, A.; Brown, A.; Hondow, N.; Wills, J.; Jenkins, G.;  
14 Doak, S., Cell Type-Dependent Changes in CdSe/ZnS Quantum Dot Uptake and Toxic  
15 Endpoints. *Toxicol. Sci.* 2015, 144, 246-258.  
16  
17 26. Hardman, R., A Toxicologic Review of Quantum Dots: Toxicity Depends on  
18 Physicochemical and Environmental Factors. *Environ. Health Perspect.* 2006, 114, 165-  
19 172.  
20  
21 27. Yong, K.; Ding, H.; Roy, I.; Law, W.; Bergey, E.; Maitra, A.; Prasad, P., Imaging  
22 Pancreatic Cancer Using Bioconjugated InP Quantum Dots. *ACS Nano* 2009, 3, 502-510.  
23  
24 28. Mo, D.; Hu, L.; Zeng, G.; Chen, G.; Wan, J.; Yu, Z.; Huang, Z.; He, K.; Zhang, C.;  
25 Cheng, M., Cadmium-Containing Quantum Dots: Properties, Applications, and Toxicity.  
26 *Appl. Microbiol. Biotechnol.* 2017, 101, 2713-2733.  
27  
28 29. Medintz, I.; Uyeda, H.; Goldman, E.; Mattoussi, H., Quantum Dot Bioconjugates for  
29 Imaging, Labelling and Sensing. *Nat. Mater.* 2005, 4, 435-446.  
30  
31 30. Mahendra, S.; Zhu, H.; Colvin, V.; Alvarez, P., Quantum Dot Weathering Results in  
32 Microbial Toxicity. *Environ. Sci. Technol.* 2008, 42, 9424-9430.  
33  
34 31. Heidelberg, J.; Paulsen, I.; Nelson, K.; Gaidos, E.; Nelson, W.; Read, T.; Eisen, J.;  
35 Seshadri, R.; Ward, N.; Methe, B.; Clayton, R.; Meyer, T.; Tsapin, A.; Scott, J.;  
36 Beanan, M.; Brinkac, L.; Daugherty, S.; DeBoy, R.; Dodson, R.; Durkin, A.; Haft, D.;  
37 Kolonay, J.; Madupu, R.; Peterson, J.; Umayam, L.; White, O.; Wolf, A.; Vamathevan,  
38 J.; Weidman, J.; Impraim, M.; Lee, K.; Berry, K.; Lee, C.; Mueller, J.; Khouri, H.;  
39 Gill, J.; Utterback, T.; McDonald, L.; Feldblyum, T.; Smith, H.; Venter, J.; Nealson, K.;  
40 Fraser, C., Genome Sequence of the Dissimilatory Metal Ion-Reducing Bacterium  
41 *Shewanella oneidensis*. *Nat. Biotechnol.* 2002, 20, 1118-1123.  
42  
43  
44  
45  
46  
47  
48  
49  
50  
51  
52  
53  
54  
55  
56  
57  
58  
59  
60

1  
2  
3 32. Hang, M.; Gunsolus, I.; Wayland, H.; Melby, E.; Mensch, A.; Hurley, K.; Pedersen, J.;  
4 Haynes, C.; Hamers, R., Impact of Nanoscale Lithium Nickel Manganese Cobalt Oxide  
5 (NMC) on the Bacterium *Shewanella oneidensis* MR-1. *Chem. Mater.* 2016, 28, 1092-  
6 1100.  
7  
8 33. Mei, B.; Susumu, K.; Medintz, I.; Mattossi, H., Polyethylene Glycol-based Bidentate  
9 Ligands to Enhance Quantum Dot and Gold Nanoparticle Stability in Biological Media.  
10 *Nat. Protoc.* 2009, 4, 412-423.  
11  
12 34. Mei, B.; Susumu, K.; Medintz, I.; Delehanty, J.; Mountziaris, T.; Mattossi, H., Modular  
13 Poly(ethylene glycol) Ligands for Biocompatible Semiconductor and Gold Nanocrystals  
14 with Extended pH and Ionic Stability. *J. Mater. Chem.* 2008, 18, 4949-4958.  
15  
16 35. Jasieniak, J.; Smith, L.; van Embden, J.; Mulvaney, P.; Califano, M., Re-examination of  
17 the Size-Dependent Absorption Properties of CdSe Quantum Dots. *J. Phys. Chem. C* 2009,  
18 113 (45), 19468-19474.  
19  
20 36. Xie, R.; Kolb, U.; Li, J.; Basche, T.; Mews, A., Synthesis and Characterization of Highly  
21 Luminescent CdSe-Core CdS/Zn0.5Cd0.5S/ZnS multishell nanocrystals. *J. Am. Chem.*  
22 Soc. 2005, 127, 7480-7488.  
23  
24 37. Wenger, W.; Bates, F.; Aydile, E., Functionalization of Cadmium Selenide Quantum Dots  
25 with Poly(ethylene glycol): Ligand Exchange, Surface Coverage, and Dispersion Stability.  
26 *Langmuir* 2017, 33, 8239-8245.  
27  
28 38. Zhang, L.; Shen, X.; Liang, H.; Chen, F.; Huang, H., Phosphine-free synthesis of  
29 ZnSe:Mn and ZnSe:Mn/ZnS doped quantum dots using new Se and S precursors. *New J. of*  
30 *Chem.* 2014, 38, 448-454.  
31  
32 39. Liu, D.; Snee, P., Water-Soluble Semiconductor Nanocrystals Cap Exchanged with  
33 Metalated Ligands. *ACS Nano* 2011, 5, 546-550.  
34  
35 40. Zheng, Z.; Saar, J.; Zhi, B.; Gallagher, M. J.; Fairbrother, D. H.; Haynes, C. L.;  
36 Lienkamp, K.; Rosenzweig, Z., Structure-Property Relationships of Amine-Rich and  
37 Membrane-Disruptive Poly(oxonorbornene)-Coated Gold Nanoparticles *Langmuir* 2018,  
38 34, 4614-4625.  
39  
40 41. Fortier, C. Preparation, Characterization, And Application of Liposomes in the Study of  
41 Lipid Oxidation Targeting Hydroxyl Radicals. University of New Orleans, University of  
42 New Orleans Theses and Dissertations, 2008.  
43  
44  
45  
46  
47  
48  
49  
50  
51  
52  
53  
54  
55  
56  
57  
58  
59  
60

1  
2  
3 42. Haldar, S.; Chatopadhyay, A., Application of NBD-labeled Lipids in Membrane and Cell  
4 Biology. In *Fluorescent Methods to Study Biological Membranes*, Springer: Berlin,  
5 Heidelberg, 2012; Vol. 13.  
6  
7 43. Feng, Z.; Gunsolus, I.; Qiu, T.; Hurley, K.; Nyberg, L.; Frew, H.; Johnson, K.;  
8 Vartanian, A.; Jacob, L.; Lohse, S.; Torelli, M.; Hamers, R.; Murphy, C.; Haynes, C.,  
9 Impacts of Gold Nanoparticle Charge and Ligand Type on Surface Binding and Toxicity to  
10 Gram-negative and Gram-positive Bacteria. *Chem. Sci.* 2015, 6, 5186-5196.  
11  
12 44. Lyons, T.; Williams, D.; Rosenzweig, Z., Addition of Fluorescence Lifetime Spectroscopy  
13 to the Tool Kit Used to Study the Formation and Degradation of Luminescent Quantum  
14 Dots in Solution. *Langmuir* 2017, 33, 3018-3027.  
15  
16 45. Were, L.; Bruce, B.; Davidson, P.; Weiss, J., Size, Stability, and Entrapment Efficiency of  
17 Phospholipid Nanocapsules Containing Polypeptide Antimicrobials. *J. Agric. Food Chem.*  
18 2003, 51, 8073-8079.  
19  
20 46. Cornelison, G.; Mihic, S., Contaminating Levels of Zinc Found in Commonly-used  
21 Labware and Buffers Affect Glycine Receptor Currents. *Brain Res. Bull.* 2014, 100, 1-5.  
22  
23 47. Verebes, G. S.; Melchiorre, M.; Garcia-Leis, A.; Ferreri, C.; Marzetti, C.; Torreggiani,  
24 A., Hyperspectral Enhanced Dark Field Microscopy for Imaging Blood Cells. *J.*  
25 *Biophotonics* 2013, 6, 960-967.  
26  
27 48. Gao, L.; Smith, R. T., Optical Hyperspectral Imaging in Microscopy and Spectroscopy—A  
28 Review of Data Acquisition. *J. Biophotonics* 2015, 8, 441-456.  
29  
30 49. Zamora-Perez, P.; Tsoutsi, D.; Xu, R.; Rivera\_Gil, P., Hyperspectral-Enhanced Dark  
31 Field Microscopy for Single and Collective Nanoparticle Characterization in Biological  
32 Environments. *Materials* 2018, 11, 243.  
33  
34 50. Peña, M. D. P. S.; Gottipati, A.; Tahiliani, S.; Neu-Baker, N. M.; Frame, M. D.;  
35 Friedman, A. J.; Brenner, S. A., Hyperspectral Imaging of Nanoparticles in Biological  
36 Samples: Simultaneous Visualization and Elemental Identification. *Microsc. Res. Tech.*  
37 2016, 79, 349-358.  
38  
39 51. Gong, K.; Kelley, D., A Predictive Model of Shell Morphology in CdSe/CdS Core/Shell  
40 Quantum Dots. *J. of Chem. Phys.* 2014, 141.  
41  
42 52. Yu, Z.; Guo, L.; Du, H.; Krauss, T.; Silcox, J., Shell Distribution on Colloidal CdSe/ZnS  
43 Quantum Dots. *Nano Lett.* 2005, 5, 565-570.  
44  
45  
46  
47  
48  
49  
50  
51  
52  
53  
54  
55  
56  
57  
58  
59  
60

1  
2  
3 **Table of Contents**  
4  
5  
6